

Astrophysics with *New Horizons*: Making the Most of a Generational Opportunity

MICHAEL ZEMCOV,^{1,2} IAIR ARCAVI,^{3,4} RICHARD ARENDT,⁵ ETIENNE BACHELET,⁴ RANGA RAM CHARY,⁶
ASANTHA COORAY,⁷ DIANA DRAGOMIR,⁸ RICHARD C. HENRY,⁹ CAREY LISSE,¹⁰ SHUJI MATSUURA,^{11,12} JAYANT MURTHY,¹³
CHI NGUYEN,¹ ANDREW R. POPPE,¹⁴ RACHEL STREET,⁴ AND MICHAEL WERNER²

¹*Center for Detectors, School of Physics and Astronomy, Rochester Institute of Technology, Rochester, NY 14623, USA*

²*Jet Propulsion Laboratory, 4800 Oak Grove Dr., Pasadena, CA 91109, USA*

³*Einstein Fellow at the Department of Physics, University of California, Santa Barbara, CA 93106-9530, USA*

⁴*Las Cumbres Observatory, 6740 Cortona Dr Ste 102, Goleta, CA 93117-5575, USA*

⁵*Observational Cosmology Laboratory, Code 665, Goddard Space Flight Center, 8800 Greenbelt Road, Greenbelt, MD 20771, USA*

⁶*U. S. Planck Data Center, California Institute of Technology, 1200 East California Boulevard, Pasadena, CA 91125, USA*

⁷*Department of Physics and Astronomy, University of California, Irvine, CA 92697, USA*

⁸*NASA Hubble Fellow, Massachusetts Institute of Technology, Cambridge, MA 02139, USA*

⁹*Henry A. Rowland Department of Physics and Astronomy, The Johns Hopkins University, Baltimore, MD 21218, USA*

¹⁰*Planetary Exploration Group, Space Department, Johns Hopkins University Applied Physics Laboratory, 11100 Johns Hopkins Rd., Laurel, MD 20723, USA*

¹¹*School of Science and Technology, Kwansei Gakuin University, Sanda, Hyogo 669-1337, Japan*

¹²*Department of Space Astronomy and Astrophysics, the Institute of Space and Astronautical Science, Japan Aerospace Exploration Agency, Sagami-hara, Kanagawa 252-5210, Japan*

¹³*Indian Institute of Astrophysics, Bengaluru 560 034, India*

¹⁴*Space Sciences Laboratory, University of California at Berkeley, Berkeley, CA, 94720, USA*

Submitted to PASP

ABSTRACT

The outer solar system provides a unique, quiet vantage point from which to observe the universe around us, where measurements could enable several niche astrophysical science cases that are too difficult to perform near Earth. NASA's *New Horizons* mission comprises an instrument package that provides imaging capability from UV to near-IR wavelengths with moderate spectral resolution located beyond the orbit of Pluto. A carefully designed survey with *New Horizons* can optimize the use of expendable propellant and the limited data telemetry bandwidth to allow several measurements, including a detailed understanding of the cosmic extragalactic background light, studies of the local and extragalactic UV background, measurements of the properties of dust and ice in the outer solar system, searches for moons and other faint structures around exoplanets, determinations of the mass of planets using gravitational microlensing, and rapid follow-up of transient events. *New Horizons* is currently in an extended mission designed to survey the Kuiper Belt Object 2014 MU₆₉ that will conclude in 2021. The astrophysics community has a unique, generational opportunity to use this mission for astronomical observation at heliocentric distances beyond 50 AU in the next decade. In this paper, we discuss the potential science cases for such an extended mission, and provide an initial assessment of the most important operational requirements and observation strategies it would require. We conclude that *New Horizons* is capable of transformative science, and that it would make a valuable and unique asset for astrophysical science that is unlikely to be replicated in the near future.

Keywords: cosmic background radiation — diffuse radiation — Kuiper belt: general — planets and satellites: detection — space vehicles — ultraviolet: ISM

1. INTRODUCTION

Astronomical observations have been performed from a wide range of locations, including the surface of the Earth, from atmospheric platforms, and in space from orbit as well as further afield like the Earth’s Lagrange points and from Earth-trailing orbits around the sun. Very occasionally, mankind has sent instruments to the outer edge of the solar system that are capable of astronomical observation (Weinberg et al. 1974; Broadfoot et al. 1977; Weaver et al. 2008). These instruments have been used to make astronomical measurements, including studies of the decrease in the light from interplanetary dust with heliocentric distance (Hanner et al. 1974; Gladstone et al. 2013), the diffuse light from the Galaxy (Toller et al. 1987; Gordon et al. 1998), the brightness of the cosmic optical background (COB; Toller 1983; Matsuoka et al. 2011; Zemcov et al. 2017) and the cosmic UV background (CUB; Holberg 1986; Murthy et al. 1991, 1999; Edelstein et al. 2000), and the UV emission from specific objects (Holberg & Barber 1985) including studies of their spectral features (Murthy et al. 1993, 2001).

Over the years, a number of missions to the outer solar system including instrumentation expressly designed to obtain astrophysical measurements have been considered (*e.g.* Mather & Beichman 1996; Bock et al. 2012; Matsuura et al. 2014; Stone et al. 2015, among others). However, these missions are costly and difficult endeavors, and require positive funding environments. A more modest strategy is to take advantage of missions during their cruise phases when they are woken for system checks and calibration campaigns. This strategy maximizes science return by taking advantage of existing assets at only a modest increase in mission risk and complexity.

NASA’s *New Horizons* mission (Stern & Spencer 2003; Weaver et al. 2008) recently performed the first detailed reconnaissance of the Pluto–Charon system. It has been approved for an extended mission to study the Kuiper Belt Object (KBO) 2014 MU₆₉ with a flyby in early 2019 and data downlink requiring approximately one year. *New Horizons* includes as part of its instrument package the Long Range Reconnaissance Imager (LORRI; Cheng et al. 2008), the Multispectral Visible Imaging Camera (MVIC), the Linear Etalon Imaging Spectral Array (LEISA; Reuter et al. 2008) and a UV spectrometer ALICE (Stern et al. 2008). In addition to their planetary imaging functions, these NH instruments can double as sensitive astronomical instruments working from the UV well into near-IR wavelengths.

New Horizons has generated a rich archival data set for both planetary studies and astronomy that is cur-

rently being analyzed. However, the instrument itself has operational capability significantly beyond its current mission, and could operate well into the heliopause. A tantalizing possibility is to use the *New Horizons* instruments for an extended mission for astrophysics where purposely-designed observations can be performed. This would help maximize the science return from the mission, and would take advantage of this unique resource. Such an opportunity will not arise again in the foreseeable future. In this paper, we outline the astrophysical studies that could be performed with the *New Horizons* instrument suite, focusing on measurements that require the exceptionally low foreground emission from the outer solar system, or the 50–100 AU separation from Earth to the spacecraft. These include measurements of the diffuse UV/optical/near-IR backgrounds away from the obscuring effects of the sun, and careful photometry science including exoplanet transits and microlensing that require an exceptionally stable platform. In Section 2 we review the primary science cases that benefit from access to the outer solar system. We assess the sensitivity and stability of the instruments using pre-flight estimates and in-flight data in Section 3. In Section 4 we outline the operational requirements of these types of measurements, and give a straw man astrophysical survey. Finally, Section 5 gives some concluding remarks and an outlook for the future.

2. ASTROPHYSICAL SCIENCE FROM THE OUTER SOLAR SYSTEM

2.1. *Measurement of the Extragalactic Background Light*

The formation of stars and galaxies in the universe is accompanied by the release of photons from both gravitational and nuclear mechanisms (Hauser & Dwek 2001; Cooray 2016). A cosmic background radiation in the UV, optical, and IR parts of the electromagnetic spectrum is therefore an expected relic of structure formation processes, and measurements of these backgrounds provide insights into those processes. Practically speaking, the extragalactic background light (EBL) at optical/near-IR wavelengths is thought to be dominated by photons released by nucleosynthesis in stars, and constraints of this stellar emission integrated over cosmic history and can yield crucial insights into a variety of astrophysical phenomena. Specifically, precise measurement of the EBL enables a cosmic consistency test wherein the integrated light from all galaxies, stars, active galactic nuclei (AGN), and other point sources is compared to the EBL intensity (Tyson 1995). Any excess component suggests the presence of new, diffuse sources of emission. Potential discoveries with profound

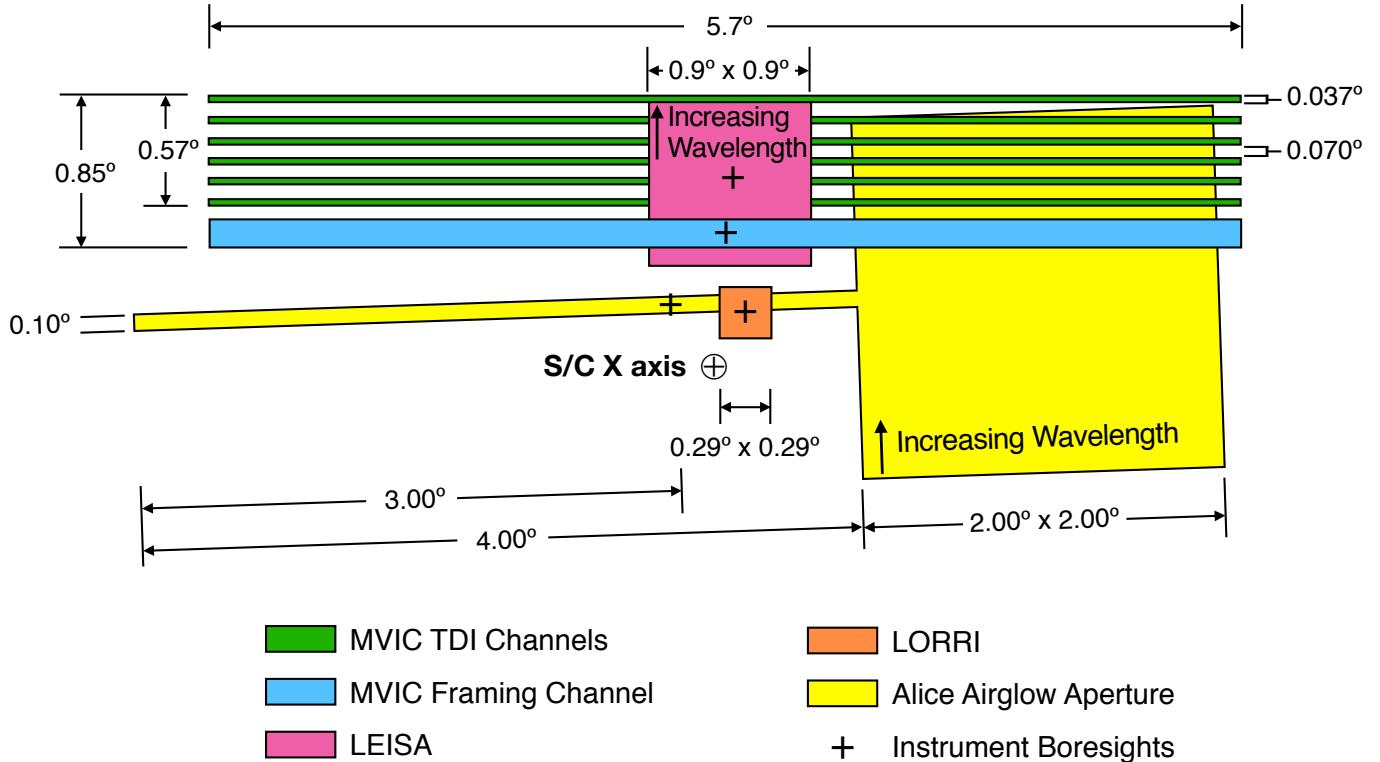


Figure 1. Layout of the focal plane of the imaging instruments on *New Horizons* (Weaver et al. 2008). LORRI has broad bandwidth, but has a relatively small footprint on the sky. MVIC observes in several colors in thin, long strips, while LEISA and ALICE have relatively large fields of view. The instrument parameters are summarized in Table 1.

implications for astronomy include the signature of diffuse recombination from the epoch of reionization (e.g. Matsumoto et al. 2005), the presence of intra-halo light in the diffuse intra-galactic medium (e.g. Zemcov et al. 2014), and diffuse photons associated with dark matter annihilation and their products (e.g. Gong et al. 2016).

In the past, direct measurements of the EBL have been complicated by the presence of bright local foregrounds, including the Zodiacal light (ZL), diffuse Galactic light (DGL), and the integrated starlight (ISL) arising from extended telescope response and faint stars (Leinert et al. 1998). Despite a great deal of interest, direct photometric measurement of the EBL has proven to be challenging, largely because the atmosphere and ZL are factors of ~ 100 brighter than the signal of interest. Though some progress has been made in accounting for these foregrounds in the optical (Bernstein 2007; Mattila et al. 2012) and into the near-IR (Gorjian et al. 2000; Wright 2001; Cambr esy et al. 2001; Wright 2004; Matsumoto et al. 2005; Levenson et al. 2007; Tsumura et al. 2013; Sano et al. 2015; Matsuura et al. 2017), small errors in this accountancy propagate to large errors on the inferred COB (e.g. Mattila 2003, 2006). As a result of mis-estimation of the foregrounds, the systematic errors of current photometric measurements of the EBL

exceed the integrated light from all galaxies outside of our own (known as the “integrated galactic light”, or IGL) by a factors of at least several. It is desirable to measure the EBL from vantage points where the ZL is not an appreciable component of the diffuse sky brightness, such as the outer solar system or above the ecliptic plane (Cooray et al. 2009).

The surface brightness of the IPD light is thought to drop with solar distance roughly as r^{-3} to levels significantly below the EBL by the orbit of Saturn (see Section 2.3). As a result, an EBL measurement from the outer solar system observing out of the plane of the ecliptic should not suffer from strong IPD light contamination. Indeed, data from the early NASA probes *Pioneer* 10 and 11 have been used to measure both the decrease in the IPD light with heliocentric distance (Hanner et al. 1974), the diffuse light from the Galaxy (Toller et al. 1987; Gordon et al. 1998), and the brightness of the COB itself (Toller 1983; Matsuoka et al. 2011) in two bands spanning 390–500 nm and 600–720 nm over heliocentric distances ranging from 1 to 5.3 AU (Weinberg et al. 1974). Due to the large field of view and poor angular resolution of the *Pioneer* photometers these measurements have uncertainties dominated by errors associated with subtracting galactic components. However, an in-

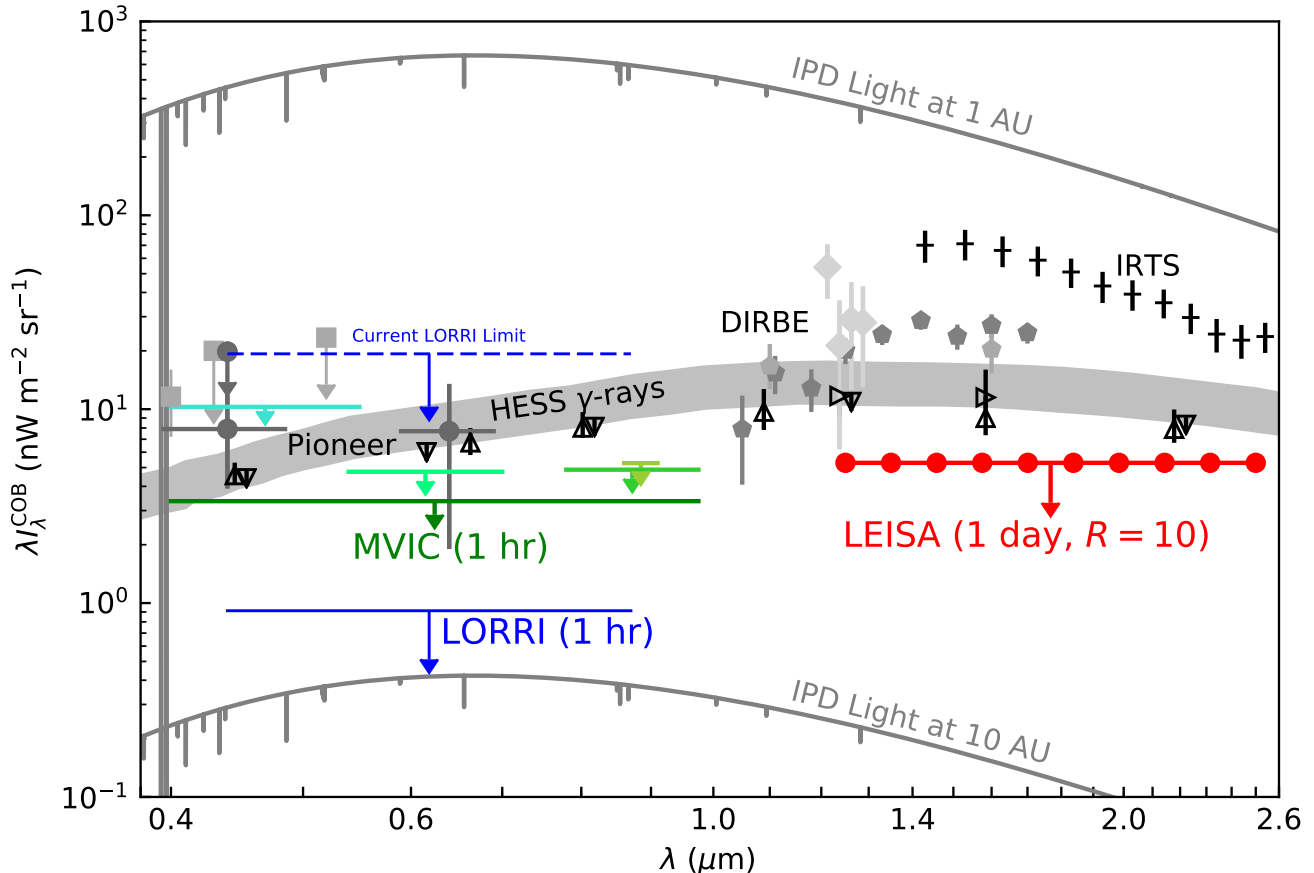


Figure 2. Measurements of the EBL surface brightness $\lambda_{\lambda}^{\text{EBL}}$ in the optical and near-IR, including existing direct photometric constraints on the EBL (filled symbols) and the integrated galactic light (IGL; open symbols). We show the expected sensitivity of LORRI in $t_{\text{int}} = 1$ hour of integration time (blue limit), MVIC in $t_{\text{int}} = 1$ hour (green limits, one for each band), and LEISA in $t_{\text{int}} = 1$ day (red limits), as well as the existing 2σ upper limit from LORRI (blue dashed; Zemcov et al. 2017). We show direct measurements of the EBL from observations using the “dark cloud” method (squares; Mattila et al. 2017), Pioneer 10/11 measurements (circles; Toller 1983; Matsuoka et al. 2011), CIBER (pentagons; Zemcov et al. 2014; Matsuura et al. 2017), combinations of DIRBE and 2MASS (diamonds; Wright 2001; Cambrésy et al. 2001; Wright 2004; Levenson et al. 2007), and IRTS (plus symbols; Matsumoto et al. 2005). The shaded region indicates the HESS γ -ray constraints on the extragalactic background light (H.E.S.S. Collaboration et al. 2013). The IGL points are compiled from the Hubble Deep Field (downward open triangles; Madau & Pozzetti 2000) and the Subaru Deep Field (upward open triangles and sideways pointing triangles; Totani et al. 2001; Keenan et al. 2010) in the optical/near-IR. Ultimately, even modest integration times could permit definitive measurements of the brightness of the EBL over 3 octaves in frequency.

strument with fine angular resolution can easily mask stars to the level that their emission is negligible, and over modest fields of view tracers of Galactic dust can be used to measure a correlation with the DGL component that can then be regressed from image. This suggests that a 10 cm-class telescope in the outer solar system, coupled with a current understanding of the galactic emission components, would be ideal for measuring the EBL.

The *New Horizons* mission includes an instrument suite that is well-suited to measurement of the EBL. LORRI is a Newtonian telescope with characteristics

including excellent pointing stability, a 20.8 cm diameter Ritchey-Chrétien telescope, an 0.3×0.3 instantaneous field of view, $1'' \times 1''$ pixels, sensitivity over a broad 440–870 nm half-sensitivity passband, and (crucially) real-time dark current monitoring. The achieved point source sensitivity of LORRI is $V = 17$ in a 10 s exposure in 4×4 pixel on-chip “rebinning” mode, making it a sensitive astronomical instrument for which the starlight that challenged the earlier Pioneer measurements can be masked out. LORRI has lately been used to measure the brightness of the EBL in the optical, yielding an upper limit that rules out some of the highest

previous measurements (Zemcov et al. 2017). However, that measurement was made on a very limited dataset that was not optimized for precise measurements of the EBL, and significant improvements are possible. In even a limited 4 hour total integration time with LORRI, uncertainties similar to those on the IGL are expected. In fact, the ultimate error from a LORRI measurement is likely limited by our knowledge of the DGL and ISL foregrounds, rather than the intrinsic sensitivity of the instrument.

Similarly, MVIC is a broad-band imaging instrument, but provides significantly more spectral information than LORRI. Compared to LORRI, each band has a long, thin field of view. This is not necessarily problematic for an EBL measurement, but the smaller aperture and narrower bandpass of the MVIC channels cause a factor of ~ 10 per pixel sensitivity penalty for measuring the average sky brightness compared with LORRI. However, averaging over the array will help, and MVIC observations remain a promising way to gain some spectral information on the shape of the EBL spectrum throughout the optical.

LEISA would make simultaneously the most interesting and challenging measurement of the EBL. The near-IR $1\text{--}3\ \mu\text{m}$ background has proven very difficult to measure from Earth, and is very interesting as the light from the earliest galaxies will be redshifted into this range. LEISA provides detailed spectral information that could be used to search for *e.g.* the spectral bump expected from Lyman emission from the galaxies that reionized the universe (Cooray et al. 2004). However, LEISA has a relatively small aperture and $R = 240$ spectral resolution, making the per pixel sensitivity poor. Significant integration time would be required to make a constraining measurement of the EBL.

2.2. Measurement of the Ultraviolet Background

The scientific interpretation of the observed cosmic ultraviolet background has been controversial for more than a quarter of a century (see *e.g.* Bowyer 1991 and Henry 1991 for contrasting viewpoints). This is primarily because it is difficult to separate the different components of the diffuse emission, particularly with imaging surveys. Any spacecraft in low Earth orbit (*eg.* *GALEX*) will be affected by airglow, while any spacecraft observing within the inner Solar System will be affected by the Lyman lines from interplanetary hydrogen and ZL at longer wavelengths. Even if we can account for these foregrounds, distant sources of astrophysical emission are difficult to separate without spectral diagnostics (Murthy 2009).

Almost all of our knowledge of the diffuse background in the spectral region longer than $1300\ \text{\AA}$ has come from *GALEX* broadband data. With only imaging data available, Murthy (2016) found that most of the diffuse radiation was due to scattered starlight, albeit with an offset of unknown origin (Hamden et al. 2013; Henry et al. 2015). However, the different components are impossible to separate photometrically, and the resulting backgrounds are highly model dependent. Measurements with the *Voyager* Ultraviolet Spectrometers (UVS), taking advantage of spectroscopic observations far from the Sun, found that the diffuse background at shorter wavelengths ($\lambda < 1200\ \text{\AA}$) is patchy with a poor correlation with the diffuse background in the NUV (Murthy et al. 2001). However, the spectral resolution of the UVS was $27\ \text{\AA}$, which rendered the separation of the diffuse background from the strong interplanetary Ly α ($1215\ \text{\AA}$) and Ly β ($1027\ \text{\AA}$) lines difficult, even from late in the mission when the intensity of the interplanetary lines had dropped by an order of magnitude. This problem is exacerbated in the extraction of the background line emission (Murthy et al. 1993, 2001).

The $9\ \text{\AA}$ resolution of ALICE is well suited to search for diffuse emission from the Galaxy, both continuum and in lines. This is both because the foreground scattered from the interplanetary HI lines is minimized through observations from the outer Solar System, and because the spectral shape of the astrophysical emission components can be used to decompose the emission. For example, emission from the Lyman and Werner bands of molecular hydrogen will extend throughout the UV in regions of high density while diffuse OVI ($1032/1038\ \text{\AA}$) emission will track the hot gas (Dixon et al. 2006). These can be used to understand the local ISM through observations of different parts of the sky. Finally, the dust scattered starlight should correlate with the positions of the emitting O and B stars. Residuals should be due to extragalactic emission at high latitudes or to a previously unknown emissive component at low galactic latitudes.

2.3. EKB Dust

Interplanetary dust particles (IDPs) are generated by several sources including comets, asteroids, and Edgeworth-Kuiper Belt (EKB) objects and range in size from $\sim 0.1\ \mu\text{m}$ up to $1\ \text{mm}$. After ejection from their parent bodies, IDPs diffuse through the solar system as they are affected by a variety of forces such as gravitation, Poynting-Robertson drag, solar radiation pressure, and solar wind drag (*e.g.* Burns et al. 1979; Gustafson 1994). As these grains encounter planetary systems, they have significant impacts on a wide range

of planetary processes such as the alteration of atmospheric photochemistry (e.g. Moses 1992; Feuchtgruber et al. 1997; Moses et al. 2000; Frankland et al. 2016; Moses & Poppe 2017), the injection of metallic species into planetary magnetospheres (Christon et al. 2015), the spatial and compositional evolution of Saturn’s main ring system (e.g. Durisen et al. 1989; Cuzzi & Estrada 1998; Estrada et al. 2015), and the production of impact ejecta clouds and/or rings from airless bodies, like planetary satellites (e.g. Verbiscer et al. 2009; Hedman et al. 2009; Poppe & Horányi 2011). An accurate understanding of the size, density, and velocity distributions of interplanetary dust throughout the solar system is critical for studies across a broad range of planetary science.

Our knowledge of the interplanetary dust distribution in the inner solar system is fairly robust, with recent model-data comparisons concluding that a significant fraction of the IDP distribution near 1 AU originates from dust emission from Jupiter-family comets with minor contributions from asteroidal and Oort Cloud cometary dust (Nesvorný et al. 2011). The three-dimensional morphology of the inner solar system IDP distribution has been mapped in detail via infrared, optical, and spectroscopic imaging (e.g., Liou et al. 1995; Hahn et al. 2002; Ipatov et al. 2008). In contrast, knowledge of the IDP distribution in the outer solar system is much more limited. In-situ measurements of outer solar system IDP densities have been taken by spacecraft such as *Pioneer* 10 and 11 (Humes 1980), *Ulysses* (Grün et al. 1995a), *Galileo* (Grün et al. 1995b), *Cassini* (Altobelli et al. 2007), *Voyager* 1 and 2 (Gurnett et al. 1997), and the *New Horizons* Student Dust Counter (Poppe et al. 2010; Szalay et al. 2013). Despite producing valuable results, these measurements have only provided information on grains with radii between $\sim 0.5 - 10 \mu\text{m}$, whereas the peak in the interplanetary dust mass flux is expected to be near $\sim 100 - 200 \mu\text{m}$. IDP spatial distributions are believed to be a strong function of grain size; for example, Figure 3 shows the (a) $0.5 \mu\text{m}$ and (b) $100 \mu\text{m}$ interplanetary dust density (including contributions from Jupiter-family comets, Oort Cloud comets, and EKB objects) from recent modeling efforts (Poppe 2016). Furthermore, since the *Voyagers* have significant out-of-ecliptic trajectories and *Pioneer* 10/11 meteoroid detectors ceased operating inside Uranus’ orbit, only the *New Horizons* Student Dust Counter (Horányi et al. 2008) has probed the EKB region itself, which is the primary source of IDPs in the outer solar system (e.g. Stern 1996; Liou et al. 1996; Vitense et al. 2010, 2012; Poppe 2016). Finally, model-data comparisons have constrained the overall production rate of

dust from the EKB and other cometary sources (Han et al. 2011; Poppe 2016); however, these limits are only based on measurements of grains $0.5-10 \mu\text{m}$ in radius and are uncertain within an order of magnitude. We require additional observations and/or constraints on the density of IPD in the outer solar system, especially those that address grains with radii from 10 to several hundred μm .

Instruments on the *New Horizons* spacecraft provide a potentially powerful but previously unexplored method for detecting and/or constraining the interplanetary dust density in the outer solar system. Solar light scattered from interplanetary dust grains can be observed by *New Horizons* as a diffuse background and, in combination with appropriate models for the dust density distribution and light scattering characteristics, can be used to place limits on the IDP distribution. To estimate the brightness scattered from the IDP distribution in the outer solar system, we have used the IPD model of Poppe (2016) which provides three-dimensional interplanetary dust densities of Jupiter-family comet, Oort Cloud comet, and EKB dust grains from $0.5 - 500 \mu\text{m}$ with $1 \text{ AU} \times 1 \text{ AU}$ resolution. We assumed the grains are comprised of astrosilicate material and used appropriate optical constants (Jäger et al. 2003) to compute the scattering phase function from Mie theory. The differential brightness of solar scattered light from each parcel of IDP density over the LORRI wavelength bandpass ($440-870 \text{ nm}$) was summed along the instantaneous line-of-sight of a virtual observer representing *New Horizons*. Figure 4 shows the predicted IDP brightness in $\text{nW m}^{-2} \text{ sr}^{-1}$ as a function of heliocentric distance for an observation at a solar elongation angle of 90° (see inset of Figure 4) along a radially outgoing trajectory (roughly approximating the trajectory of *New Horizons*). In the inner solar system ($r < 5 \text{ AU}$), scattered IDP light is on the order of $1-50 \text{ nW m}^{-2} \text{ sr}^{-1}$ arising mainly from Jupiter-family comet dust, consistent with *Pioneer* 10 photopolarimetry measurements (Hanner et al. 1974). In the outer solar system, the surface brightness slowly tapers off, averaging approximately $0.01-1 \text{ nW m}^{-2} \text{ sr}^{-1}$ mainly from contributions by Oort Cloud cometary dust and EKB dust. Importantly, the uncertainty for these model predictions is large, as denoted by the shaded region in Figure 4. Measurements of the scattered IDP brightness by LORRI outside of 40 AU have the potential to constrain the contributions from Oort Cloud cometary dust and EKB dust to the outer solar system IDP distribution over the summed range of sizes ($0.5-500 \mu\text{m}$), representing a powerful new constraint on the outer solar system dust density.

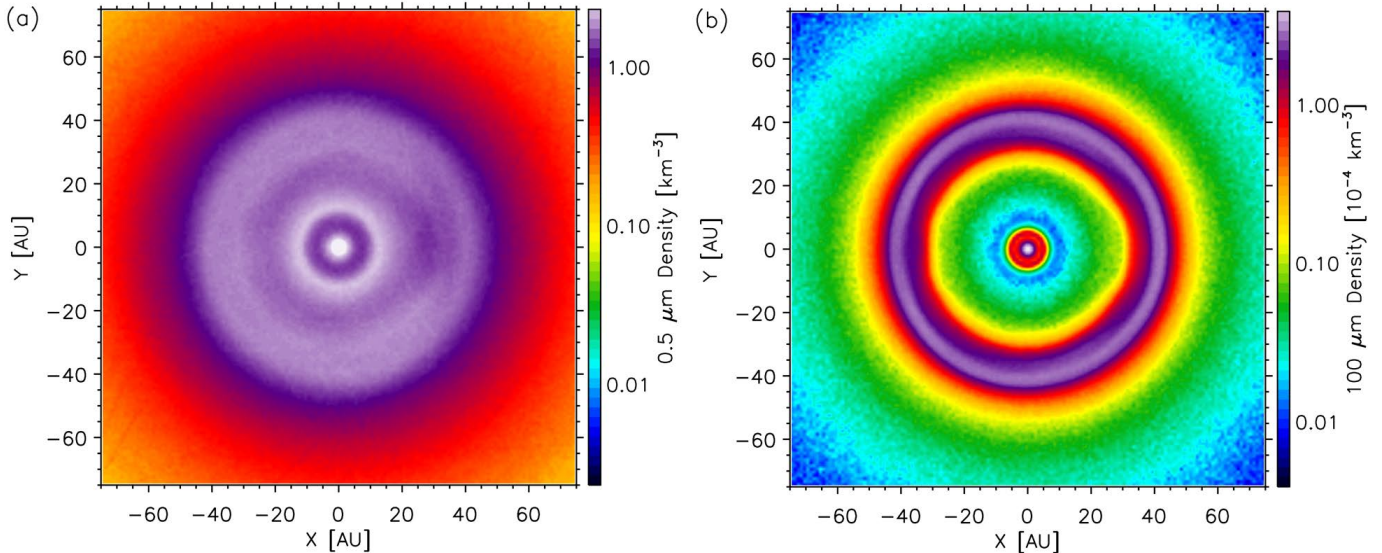


Figure 3. A model for the density distribution of (a) $0.5 \mu\text{m}$ and (b) $100 \mu\text{m}$ interplanetary dust particles in the ecliptic plane based on that presented in Poppe (2016). Though the surface brightness of the light reflected by dust drops as $1/r_{\odot}^2$, a density enhancement is expected in the outer solar system near 40 AU where LORRI is capable of making measurements in reflection.

A previous suggestion of direct detection of light scattering from interplanetary dust in the outer solar system comes from work by Chary & Pope (2010), who inferred the possible presence of high albedo ($a \sim 1$), icy dust between ~ 20 – 80 AU based on discrepancies between integrated galaxy light (IGL) and the EBL in the mid-IR. They estimated the IDP brightness at optical wavelengths in the outer solar system to be $\sim 25 \text{ nW m}^{-2} \text{ sr}^{-1}$, several orders of magnitude higher than predicted by our model. Chary & Pope (2010) theorized that such icy, high albedo dust could be shed from comets at distances far from their perihelia (such activity has been detected in Jupiter-family comets Kelley et al. 2013 and could also apply to Oort Cloud comets). If the IDP brightness in the outer solar system is truly this bright, *New Horizons* will be able to detect it, and this information can be used to add an appropriate icy dust grain composition to the current EKB dust models. Intriguingly, the presence of an icy halo of dust in the outer solar system at unexpectedly high densities may not necessarily conflict with *in-situ* measurements by dust detectors (Humes 1980; Poppe et al. 2010) given that icy grains born in the outer reaches of planetary systems may perhaps migrate outwards rather than inwards due to mass loss via photodesorption and/or charged particle sputtering and subsequent ejection via stellar (or solar) radiation pressure (i.e., so-called “beta meteoroids”; Grigorieva et al. 2007). If *New Horizons* provides evidence for isotropic, icy dust grains, current interplanetary dust dynamics models will be revised by adding an additional component of isotropic, icy dust released from Oort Cloud comets and EKB objects.

2.4. Transits in Exoplanetary Systems

Measurements of exoplanet transits can provide a great deal of information about exoplanetary systems (Rice 2014). In the transit method, the light curves of stars hosting exoplanets are photometrically monitored for long periods, and occultations of the star by the planet (or vice versa) are sought. The duration, shape, and repetition frequency of the resulting dip in the star’s light curve can yield a great deal of information about the planetary system. This is the motivation for instruments like *Kepler* Borucki et al. (2010), which photometrically monitored $> 10^5$ stars to search for exoplanets in our galaxy.

Though by now many thousands of planetary systems have been identified with this method, its promise has only begun to be realized. In addition to wider survey fields, precision photometry could, in principle, allow detection of finer features like rings and moons around these planets (Heller 2017). Several methods have been proposed to search for these faint structures, including transit time variations (TTV) and transit duration variations (TVD; see Kipping et al. 2010 for a review), as well as the orbital sampling effect (OSE; Heller 2014). All of these methods rely on both precision photometry of the star, as well as measurements over many orbits of the moon’s parent planet to sample different parts of the moon’s orbital phase. These requirements mean that not only must the photometer be very stable, but that observations occur over a long time baseline to capture the system in different orbital configurations (Heller et al. 2016a,b).

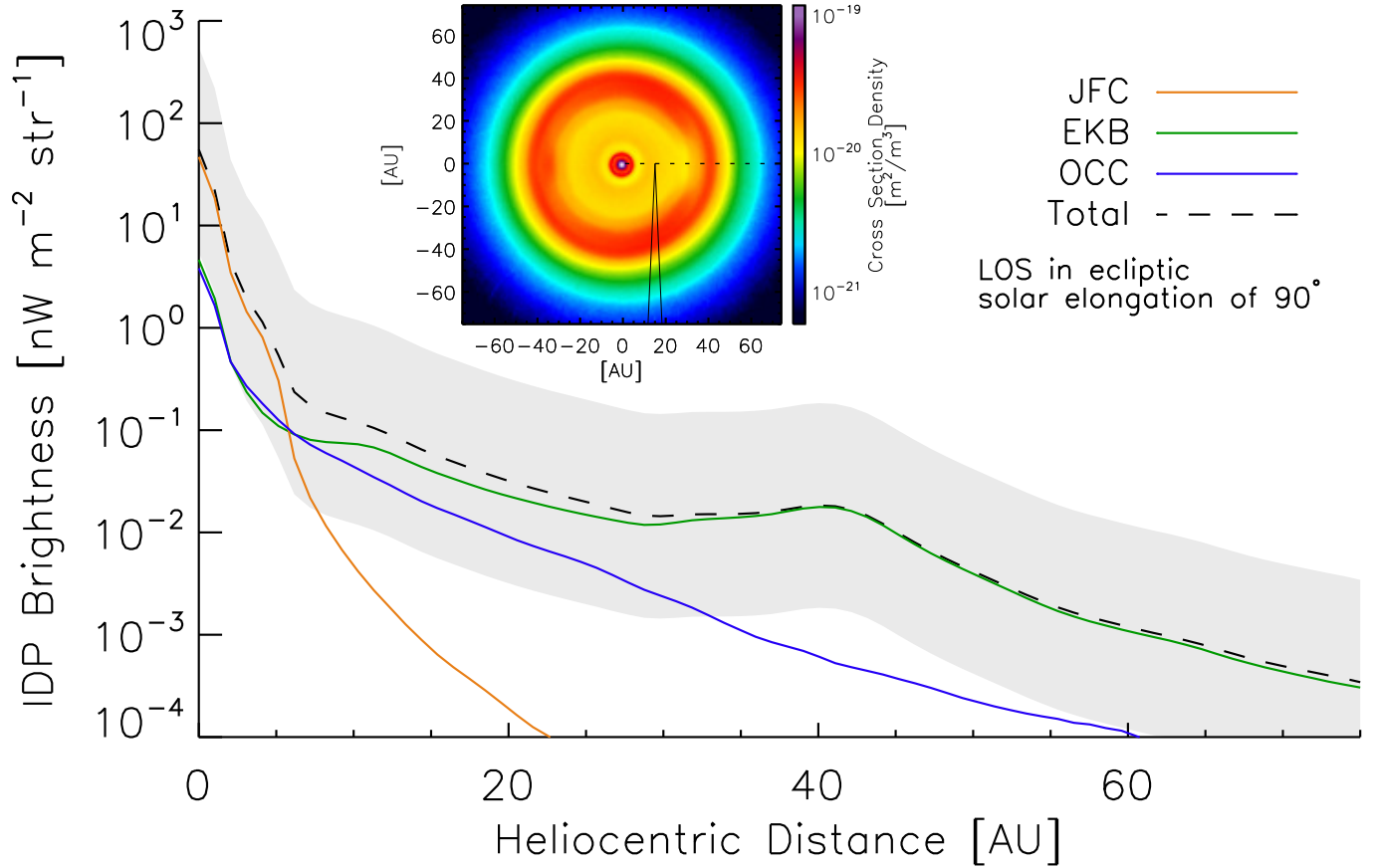


Figure 4. The estimated IDP brightness as a function of heliocentric distance for an observer along a radially outward trajectory with solar elongation angle of 90° . Inset: The IDP cross sectional density (m^2/m^3) along with the notional observer.

Further, measuring the occultation timing variation between the orbit of Earth and from many tens of AU distances could also help improve models of transiting planets, and possibly help us understand the dynamics of the planet’s orbits through phase shifts that can allow us to deduce the rotation of the exoplanet orbits. The details of the timing of light curves of exotic systems such as Kepler KIC 8462852 (Boyajian et al. 2016) could help resolve the mystery of the structure of the occulting material.

A vantage point in the outer Solar system gives a quiet, stable platform from which to perform measurements at the required $\delta F/F \sim 10^{-5}$ level. Measurements of known transiting systems with LORRI over the long time baselines afforded by an outer solar system cruise might allow detection of moons around large planets and exoplanetary rings. There are several advantages to using *New Horizons* for these type of measurements, including: (i) the similarity of the LORRI detector with the *Kepler* detectors, which have shown remarkable stability on-orbit (Caldwell et al. 2010); (ii) a well-understood point spread function, which allows accurate photometry of sources (Morgan et al. 2005; No-

ble et al. 2009; Cheng et al. 2010); (iii) the lack of ZL variations, giving an extremely stable image background in measurements of the same field separated by long periods; and (iv) the quiet instrument environment, in which (presumably) most of the instruments would be in a quiescent state, and *e.g.* thermal transients from solar heating would be entirely absent.

Another issue that observations with a long time baseline can help address is ephemeris drift, which is the accrued uncertainty in the position of an exoplanet between discovery and detailed follow-up observations. For example, if a transiting system is discovered with *Kepler* or *Spitzer* circa 2015, for observations with *e.g.* the coronagraph on *WFIRST* a decade later (or *LUVOIR* or *HabEx* in the 2030s) the uncertainty in the transiting systems orbit accrues to the point the planet may be lost. Transit timing data with *New Horizons* in the early 2020s could help bridge the gap between observations.

The launch of the Transiting Exoplanet Survey Satellite (*TESS*) in 2018 will lead to the discovery of thousands of new transiting exoplanets around bright stars. These planets will allow a range of follow-up observations, so in this sense will be much more valuable than

Kepler and *K2*. However, due to the photometric precision of *TESS* and the relatively short observing baseline (compared to *K2* or *Kepler*), the ephemerides of most *TESS*-discovered planets will become “stale” very quickly. Figure 5 shows the uncertainty in the mid-transit time of all simulated *TESS*-planets with two or more transits, one year after the last transit is observed by *TESS* during the primary mission. Out of approximately 1600 2-minute cadence planets expected from *TESS*, 400 will have 1σ uncertainties on the mid-transit time greater than 1 hour, and 100 greater than 2 hours. For the 30-minute cadence, out of 3400 planets, 1400 will have uncertainties greater than 1 hour and 600 greater than two hours.

Ground-based resources will not be able to reliably recover transits shallower than $\sim 1\text{--}3$ mmag. Even for deeper transits, recovery of transits from the ground is very challenging if the mid-transit time uncertainties (1σ) are greater than ~ 4 hours, especially, when the Earth’s diurnal schedule and weather patterns are coupled into the observability window functions. To recover the ephemerides of these planets for scheduling future observations, such as transit and eclipse spectroscopy with the *JWST*, a space-based observatory is needed.

TESS will discover over 500 planets with periods longer than 27 days that show at least two transits in the *TESS* light curves and have a total signal-to-noise ratio (SNR) greater than 7.3 (Sullivan et al. 2015). By also exploiting single-transit events, this yield can be more than doubled, with potential to discover up to 900 *additional* planets with periods > 27 days. In order to determine which of these single-transit events are true planets, the usual vetting process will need to be supplemented with extra steps. One of these steps is to capture a second transit. This will happen after an ephemeris has been obtained using radial velocity (RV) monitoring of the system, and constraints from any additional, multi-transiting planets in the system. However, the uncertainty on the next mid-transit time is likely to be at least several hours, making it difficult to ensure a transit is captured from the ground. A space-based observatory such as *New Horizons* could be critical to the confirmation of numerous single-transiting *TESS* planets.

There are currently three space-based observatories that could be used for the long-term monitoring and recovery of transits: *Spitzer*, *MOST* and *CHEOPS*. The *MOST* space telescope is not currently funded, and functions only if a user can purchase time. *MOST*’s photometric precision is also lower than even that of *TESS* (making it difficult to use for shallower single-transit events), and becomes equivalent to that of ground-based facilities for targets fainter than V mag of 11. The Eu-

ropean Space Agency is launching CHAracterising ExO-Planets Satellite (*CHEOPS*) in late 2018 to obtain optical transits and phase curves of exoplanets, but only 20% of the time is available outside the guaranteed time, and guest observations may not be accomplished if the observations conflict with the guaranteed time observations of the science team. Additionally, large portions of the *TESS* footprint is out of the field-of-view for *CHEOPS*, and *CHEOPS*’s orbit is similar to *HST*’s orbit, meaning that observations will be periodically interrupted by the Earth – making timing measurements more complicated and shorter transit events may be missed. Finally, *Spitzer* is only funded through spring of 2019, so its usefulness for *TESS* follow-up is limited to a few months at most.

An extended *New Horizons* mission that can observe *TESS* planet transits throughout the sky could be critical to the rescue of transit ephemerides for future observations and to the search and confirmation of new *TESS* planets, thus uniquely enhancing the *TESS*’ mission science return.

2.5. Breaking Mass Degeneracies in Microlensing

Like exoplanet transits, microlensing of distant stars by foreground massive objects is a time-domain technique wherein photometric monitoring of background stars reveals a distinctive brightening and fading, and where abrupt changes in the lightcurve can betray the presence of companions to the (invisible) lensing body. Typically, stars in our galaxy’s Bulge are monitored as this maximizes the number of potential targets per area on the sky. Microlensing is the most effective method for finding exoplanets beyond the snow line of their stars, where the sensitivity of other planet discovery techniques drops off rapidly: gravitational reflex motions are small, the probability of transit is low, planets are cold, and the light available to reflect to telescopes at Earth is small. To date, 53 planetary systems detected by microlensing have been published¹. Since the technique does not rely on receiving any light from the lens itself, it is uniquely sensitive to *any* massive body, including compact objects (Wyrzykowski et al. 2011) and even free-floating planets (Mroz et al. 2017).

The mass and distance of a lensing object are degenerate in point source, point lens events, but this can be broken if microlensing parallax can be measured (Gould 1992; Buchalter & Kamionkowski 1997), by observing the same event from multiple, widely-separated, locations. For events with extreme high magnification, the separation required is as small as the Earth’s radius

¹ <https://exoplanetarchive.ipac.caltech.edu>

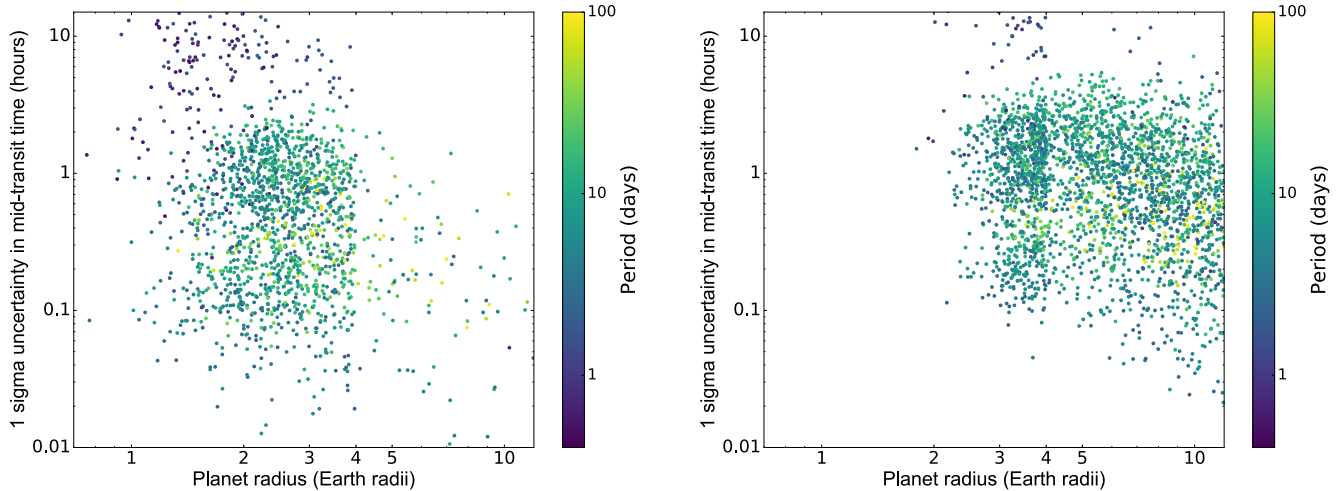


Figure 5. The uncertainty in mid-transit time for simulated planets one year after *TESS* observes them. *Left*: short cadence (2 minutes). *Right*: Long cadence (30 minutes).

(Gould et al. 2009), but these are rare. More commonly, parallax is measured either because the event is long enough for the Earth to move in its orbit appreciably during the event (Muraki et al. 2011, e.g.) or by obtaining simultaneous light curves from Earth- and space-based observatories such as *Spitzer* and *K2* (Dong et al. 2007; Yee et al. 2015; Street et al. 2016; Zhu et al. 2017a, e.g.).

In contrast to those missions however, it is unlikely to observe simultaneously the same microlensing event from Earth and *New Horizons*. A lensing object of mass M_L at distance D_L from Earth deflects the light of a source at distance D_S around itself with a characteristic Einstein radius, $r_E = \sqrt{\frac{4GM_L D}{c^2}}$, where $D = \frac{D_L D_{LS}}{D_S}$ and D_{LS} is the distance between the lens and source (see Fig. 6). To give an illustrative example: for a $1 M_\odot$ object at 4 kpc lensing a source at 8 kpc, $r_E = 4.0$ AU. Projecting this radius to the plane of the observer (\tilde{r}_E) gives a guide to the region within the Solar System from which the event can be seen; any observer within this region will see the object lens the source star, though the maximum magnification and time of peak will vary as a result of the different closest approach separations observed from different locations. For our stellar-mass lens example $\tilde{r}_E = 8.1$ AU, while for a $10 M_\odot$ black hole $\tilde{r}_E = 25.5$ AU. However, the lensing magnification drops off rapidly for observers outside this radius. Since *New Horizons*' separation from Earth is much larger than the projected Einstein radius of any plausible lens, the magnification it would experience while the event is seen lensed from Earth would be undetectably small. Conversely, though, *New Horizons* will discover lensing events unknown on Earth.

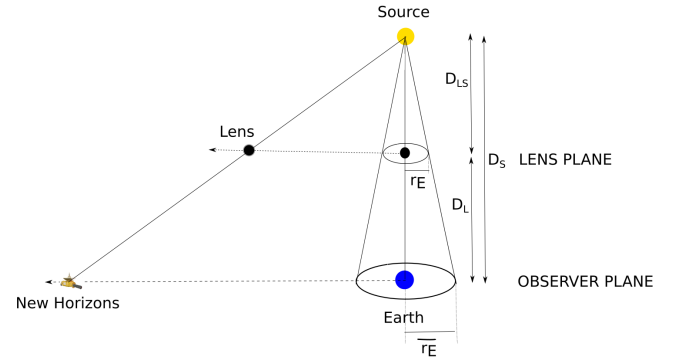


Figure 6. Schematic diagram of the (simplified) geometry of a lensing event as seen from Earth and *New Horizons*, defined such that the Earth-source line is considered to be fixed and the lens moves relative to it. The lensing object is shown as a black dot at the time of maximum magnification as seen from both Earth and *New Horizons*.

New Horizons' extraordinary velocity, currently 14.22 km s^{-1} , is close to half of the average orbital velocity of the Earth ($\sim 30 \text{ km s}^{-1}$). In the course of a typical event lasting ~ 60 days, the spacecraft moves $7.4 \times 10^7 \text{ km}$ or $\sim 0.5 \text{ AU}$, on a trajectory where the major component of motion is perpendicular to the Galactic Plane. By comparison, the Earth travels $\sim 1 \text{ AU}$ around its orbit and $\sim 0.3 \text{ AU}$ perpendicular to the Galactic Plane within the same time frame. The trajectory of *New Horizons* may therefore produce a significant parallax signature which might be detected from *New Horizons* light curves without additional data, breaking the degeneracies and allowing the events to be characterized.

Once a lensing event has been seen from Earth, the relative motion of the lens carries it out of alignment

with the original observer. For a small fraction of lens relative trajectories, the lens could in principle subsequently cross the line of sight to the source from *New Horizons*, so that the spacecraft would experience a different lensing event caused by the same lens, after a delay of ~ 2.6 yrs, for lenses moving with typical relative velocities of ~ 120 km s $^{-1}$. A small number of events discovered at one observing platform might therefore be followed up from the other. For events where constraints on parallax can be derived from Earth-bound observations (for instance), one component of the parallax ($\pi_E = AU/r_E = (\pi_{E,N}, \pi_{E,E})$) is typically measured with far greater precision than the other. Nevertheless, if the first observer can place *some* constraints on the event parallax, this information could be used to pre-select targets most likely to exhibit a lensing event from the second platform, and those follow-up observations would provide much tighter constraints on the lens trajectory and event model and hence on the lens' physical parameters.

Companion objects in the lensing system can cause lightcurve anomalies that are most likely to occur if the projected separation of the companion from the primary lens at the time of the event happens to coincide with the primary lens' Einstein radius. Observations of an event therefore act to probe for companions at specific locations in the plane of the lens, which can be mapped (*e.g.* Tsapras et al. 2016). Naturally, during the delay between events caused by the same lens as seen from both Earth and *New Horizons*, any companion objects move in their orbits around the lens host star. Observations of a second lensing event therefore effectively probes more of the lens plane, improving our sensitivity to lens companions. It could also be used to detect binary source stars, as their orbit would subtly change their lens-source-observer alignment between events and hence affect the observed magnification.

The probability of microlensing occurring is intrinsically low, but highest in the direction of the dense star fields of the Galactic Bulge ($\Gamma = 4.60 \pm 0.25 \times 10^{-5}$ star $^{-1}$ yr $^{-1}$ at $|b| \sim -1.4$ and $2.25 < l < 3.75$, for sources with $I < 20$ (Sumi & Penny 2016). Microlensing programs therefore necessarily observe in highly crowded fields, and require reasonably high spatial resolution instruments. For this reason, *New Horizons*' LORRI telescope is best suited to this science.

LORRI offers a spatial resolution of 1×1 arcsec and a single wide optical passband (350–850 nm). While its pixel scale is somewhat larger than current ground-based optical surveys (*e.g.* OGLE has 0.26 arcsec/pixel resolution) it is comparable with some of the telescopes used

by ground-based follow-up teams (*e.g.* MicroFUN²). The larger pixel scale means that the lensed source will suffer somewhat higher blending with nearby stars, but this can be determined by modeling the event lightcurve provided it is sampled at a range of different magnifications. LORRI's wide passband is beneficial to harvesting as much light as possible from the relatively faint source stars ($I < 20$ mag) and the photometric precision required for microlensing is relaxed compared with transit measurements: typically $\sim 1\%$. It's reasonably wide field of view (0.29×0.29 sq.deg), which is similar to that of the 1st generation microlensing surveys, could be used to monitor multiple events at once.

In addition to a well-sampled lightcurve, multi-band photometry is required to determine the spectral type and distance of the source star in a microlensing event. The Ralph-MVIC instrument offers 5 passbands in 400–975 nm that could be used for this purpose, though with lower spatial resolution (4.1×4.1 arcsec). While non-optimal in these crowded fields, this resolution is similar to that of *Kepler*, which has provided lightcurves of microlensing events thanks to advanced detrending techniques (Zhu et al. 2017b). Ralph-MVIC has a brighter limiting magnitude than LORRI ($R = 15.3$ mag at current maximum integration time), owing to its smaller aperture, and an asymmetric field of view. This instrument is therefore better suited to a more targeted strategy, obtaining low-cadence multi-band imaging of selected bright events during their peaks.

We can estimate the number of events which *New Horizons* could detect from the distribution of baseline source star magnitudes alerted each year by the ground-based surveys. Of 1834 events found by OGLE in 2017, 824 (44.9%) had a baseline (*i.e.* unlensed) magnitude $I < 18.6$ mag, LORRI's limiting magnitude in a 30s integration. 46 events had a baseline brighter than Ralph-MVIC's limiting magnitude. This figure underestimates the number of events which could be observable to Ralph-MVIC however, since color observations are primarily required over the peak of an event when the target is brighter. While ground-based surveys cover a footprint that is much larger than *New Horizons* could monitor, they have also shown that events are not uniformly distributed across the Bulge (Poleski 2016); $\sim 41\%$ are discovered within a central $\sim 3.3 \times 3.3^\circ$ region.

2.6. Transient Follow-Up

The study of astronomical transients touches on many areas of physics. The explosions of massive stars as supernovae reveal the physics of matter under intense den-

² <http://www.astronomy.ohio-state.edu/~microfun/>

sities and temperatures, and provide insights into shock physics, the origins of the elements, and the sources of extra-galactic neutrinos, high energy particles and gamma-rays. Rapid follow-up of gravitational wave detections has only begun, but the discovery of the first kilonova is already shedding light on the neutron star equation of state, the physics of their mergers, and the resulting r -process nucleosynthesis and its role in producing the heavy elements.

Many of these phenomena occur with timescales ranging from a few days to a few months. Occasionally, critical phases of these events, or even entire events, are missed due to the relative positions of the Earth, the Sun, and the event being studied. One notable example is the recent electromagnetic counterpart to the gravitational wave event GW170817 (Abbott et al. 2017a,b), which has allowed us to constrain the ejecta properties and the associated nucleosynthesis, study the environment of the neutron star merger, and for the first time, use gravitational wave events as “standard sirens” (Abbott et al. 2017c), providing a completely new probe for cosmology. A fact often missed is that had GW170817 occurred just one week later, it would have been unobservable to Earth-based ultraviolet, optical and infrared telescopes, the electromagnetic counterpart would not have been found, and the incredible insights gained from this event would have been lost.

More events need to be observed in order to settle the disputed nature of some of the emission components, and to improve the uncertainties in the inferred cosmological parameters. The expected rate of binary neutron star merger detections is uncertain, due to both order-of-magnitude uncertainties in the intrinsic rates of such mergers and uncertainties in the final sensitivity of the LIGO and Virgo detectors. However, when LIGO and Virgo reach design sensitivity, the event rate could be between a few per year and a few per week (Abbott et al. 2017a). Because LIGO and Virgo are not sensitive the Earth’s position relative to the sun and can detect gravitational waves from any position in the sky, a large fraction of these events will be unobservable to any optical, ultraviolet or infrared telescope in existence, except one far from Earth. For approximately half of the year, *New Horizons* is opposite the sun from Earth and so has exclusive access to large parts of the sky.

Several of the instruments that found the electromagnetic counterpart to GW170817 have very similar properties to those of LORRI. Despite the small field of view compared to the LIGO and Virgo localization regions (of tens of square degrees) the counterpart was quickly identified by pointing telescopes to a list of known galaxies in the localization region (Nissanke et al. 2013; Singer

et al. 2016; Gehrels et al. 2016; Arcavi et al. 2017a). This same strategy could be used with *New Horizons* when a gravitational wave detection of a binary neutron star, or neutron-star black-hole merger, is detected on the opposite side of the sun from Earth. Even though the data could not be transmitted to us immediately, detecting the counterpart in retrospect, and obtaining even a single flux measurement, would be extremely useful for many of the above science cases. Additionally, *New Horizons* could be used to follow events discovered close to their observability limit, such as was the case with GW170817. In this scenario, the counterpart would be identified by other telescopes and *New Horizons* would be used to image it once it can no longer be observed from Earth or Earth orbit. The point source sensitivity of LORRI is adequate to detect the kilonova associated with GW170817 that peaked at $r \sim 17$ (Arcavi et al. 2017b; Drout et al. 2017; Pian et al. 2017; Valenti et al. 2017). Additional high-value and time-critical transients could also be observed by *New Horizons*. For example, even single-epoch flux measurements of particular supernovae can be critical in bridging observing gaps due to sun constraints.

3. SENSITIVITY AND STABILITY ESTIMATES

To determine the capability of *New Horizons* for astrophysical observations, it is necessary to estimate the sensitivity of the instrument to both unresolved and resolved emission. In Table 1 we summarize the parameters of LORRI, Ralph, and ALICE based on published pre-launch and in-flight assessments of their performance (Morgan et al. 2005; Conard et al. 2005; Weaver et al. 2008; Cheng et al. 2008; Reuter et al. 2008; Stern et al. 2008; Noble et al. 2009; Cheng et al. 2010; Zemcov et al. 2017). Based on these parameters, we can derive simple point source and extended emission sensitivities that take into account the instrument performance (Bock et al. 2013).

The surface brightness sensitivity estimate for LORRI listed in Table 1 is based on in-flight performance that the *New Horizons* team has measured. Zemcov et al. (2017) performed a detailed study of the LORRI performance in the context of astrophysical observations of diffuse surface brightness, and find performance figures in agreement with the LORRI team.

The sensitivity characteristics of ALICE are given in Stern et al. (2008) and summarized in Figure 7. The instrumental Lyman- α foreground has been declining steadily, and recent unpublished ALICE observations show that the instrument is currently at a level such that we can expect to obtain spectra with astrophysical

Table 1. A Summary of the Characteristics of New Horizons Instruments Capable of Astrophysical Observations.

Parameter	LORRI	Ralph-MVIC	Ralph-LEISA	ALICE
Instrument Type	Single Band Imager	Multi-band Imager	Imaging Spectrometer	Spectrometer
Wavelength Range	350–850 nm	400–975 nm	1.25–2.5 μm	470–1880 \AA
Spectral Resolution	1.2	1.2 (pan & framing), 3.2 (blue), 3.9 (red), 4.5 (IR), 17.7 (CH4)	240	133
Spatial Resolution (arcsec^2)	1.0×1.0 (or $4.3 \times 4.3^{\text{a}}$)	4.1×4.1	12.8×12.8	1000×1000
Number of pixels	1024×1024 (or $256 \times 256^{\text{a}}$)	Framing channel $2 \times 5000 \times 32$; all others 5000×32	256×256 (~ 1 pixel per spectral element)	1024×32
Field of View (sq. deg.)	0.29×0.29	5.7×0.037	0.9×0.9	$0.1 \times 4.0 + 2.0 \times 2.0$
Telescope Primary Aperture (cm)	20.8	7.5	7.5	4×4
Optical Beam FWHM (arcsec)	0.5	2.0	18.1	-
Operating Temperature (K)	200	200	100	290
Data Size (Mb frame $^{-1}$)	16.8 (or 1.05^{a})	17.9	1.0	0.5
Maximum Integration Time (s)	30	10	4	600
Point Source Sensitivity $^{\text{b}}$	$V = 18.6$ in 4×4 pixel bins $^{\text{a}}$	$R = 15.3$	$J = 10.6, H = 9.8, K = 8.9$	-
Per Pixel Surface Brightness Sensitivity $^{\text{b}}$	$2.2 \times 10^3 \text{ nW m}^{-2} \text{ sr}^{-1}$	$3.8 \times 10^4 \text{ nW m}^{-2} \text{ sr}^{-1}$	$6.0 \times 10^4 \text{ nW m}^{-2} \text{ sr}^{-1}$	1 Rayleigh
Characteristic Surface Brightness Sensitivity $^{\text{b}}$	$10 \text{ nW m}^{-2} \text{ sr}^{-1}$	$95 \text{ nW m}^{-2} \text{ sr}^{-1}$	$750 \text{ nW m}^{-2} \text{ sr}^{-1}$ in $R = 10$ bins	$0.9 \text{ nW m}^{-2} \text{ sr}^{-1}$ at $R = 133$

^a Deep observations are typically performed in 4×4 pixel binning mode to improve sensitivity.

^b 1σ at maximum integration time (as discussed in Section 4.3). Red channel specifications listed for MVIC.

as opposed to instrumental information in coming years (Murthy, private communication).

MVIC is well characterized, and has observed a variety of astronomical objects during cruise phase (Olkin et al. 2006; Howett et al. 2017). As a result, its noise properties and radiometric calibration are quite well understood, and are summarized in Table 1. As a check of the predictions given in Reuter et al. (2008), we performed an analysis of the 2006 observations of Asteroid 2002 JF56, and found array standard deviations well matched to the notional noise levels in calibrated data. As predicted, the effective surface brightness sensitivity is worse than that for LORRI, largely due to the combination of smaller aperture, narrower spectral bandpass, and shorter maximum integration time.

To assess the sensitivity of LEISA, we have studied data taken on the star Vega (αLyr) in late 2008. In this observation, the star was scanned across the dispersive direction of the imaging array with $t_{\text{int}} = 0.59$ s per resolution element. The total observation time was 198 s. The data are calibrated to I_λ in $\text{erg s}^{-1} \text{ cm}^{-2} \text{ sr}^{-1} \text{ \AA}^{-1}$ using the nominal calibration factor for LEISA (derived, in part, from these same data). In our analysis, we performed aperture photometry of the star image in each frame, using a circular aperture of $r = 2$ pixels and an

outer annular aperture of $2 < r < 4$ pixels. We then subtract the Hubble Space Telescope CALSPEC Flux Standard for αLyr and compute the standard deviation of the residuals (Bohlin 2014) to determine $\sigma(I_\lambda)$. From this, we estimate $\sigma(\lambda I_\lambda)$ to be $< 6.7 \times 10^4 \text{ nW m}^{-2} \text{ sr}^{-1}$ per pixel in a 4 s integration and assuming the FWHM of the beam is $1.44 \times$ the pixel resolution (Reuter et al. 2008), which is consistent with the published estimate of $6.0 \times 10^4 \text{ nW m}^{-2} \text{ sr}^{-1}$ per pixel.

The instrument most useful for exoplanet investigations is LORRI, where the primary parameter of interest is the photometric stability of the instrument. To help assess the photometric stability of LORRI, we have used data from the Pluto cruise phase of the *New Horizons* mission centered on $(\alpha_{\text{J2000}}, \delta_{\text{J2000}}) = (18^{\text{h}}02^{\text{m}}.6, -14^{\circ}37'.8)$. This field happened to be the position of Pluto as viewed from *New Horizons* between 2012 and 2014 while the mission was in-bound from about the orbit of Uranus. Pluto was still a faint object in these images, and many stars are visible in the images. An example image is shown in Figure 8.

The data discussed here were reduced and calibrated using the pipeline described in Zemcov et al. (2017). As in that work, these observations are “found data” that are not ideal for this type of stability characteriza-

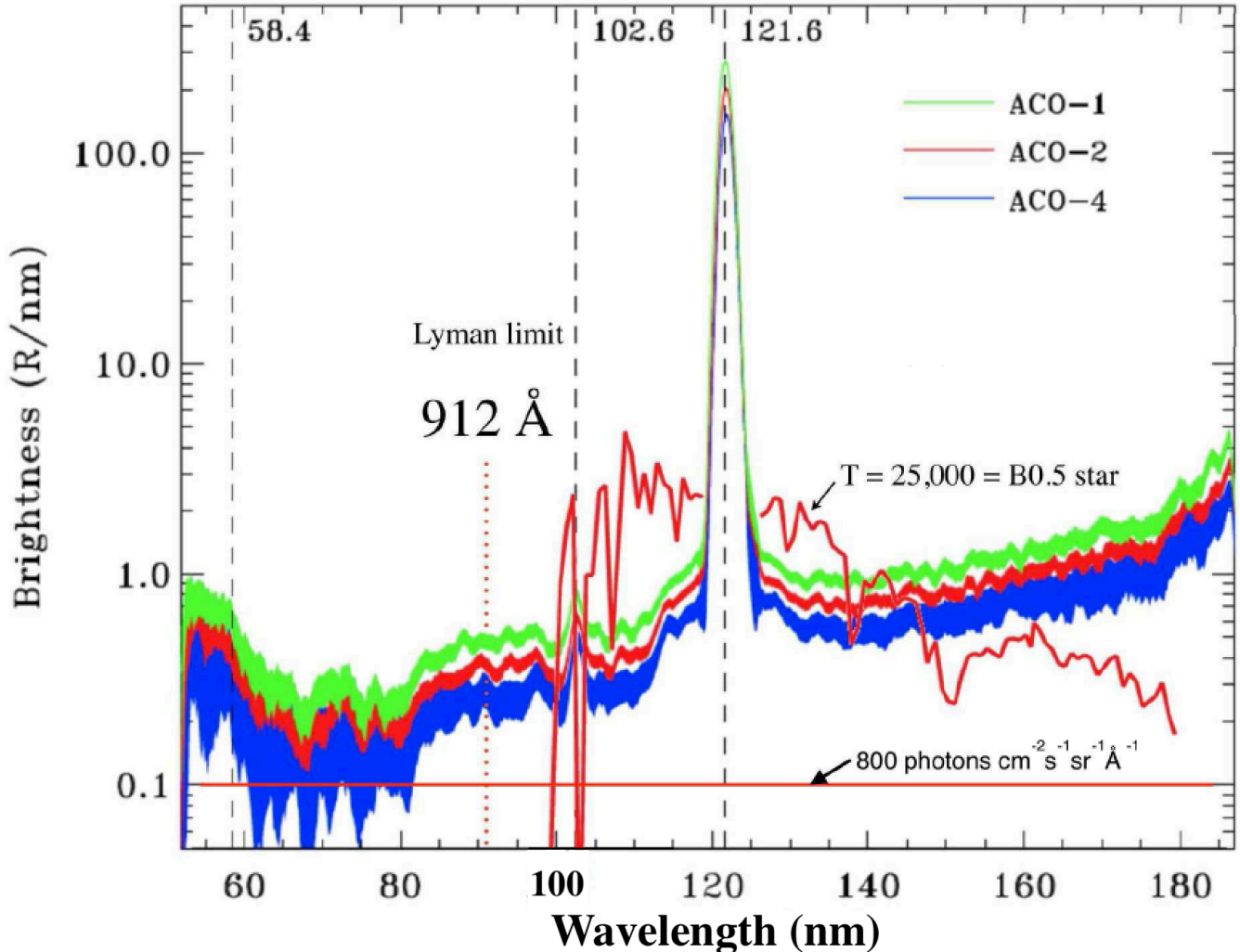


Figure 7. The three published ALICE UV spectra, showing the decline in surface brightness with increasing heliocentric distance observed in the same field (Gladstone et al. 2013). Also appearing is the spectrum of a hot star, with a vertical scale exaggerated by a factor 1.5 to bring out more clearly the stellar spectral features that we hope to detect (or, more dramatically, to fail to detect) in ALICE observations of the cosmic background. A brightness of 0.1 R/nm corresponds to 0.01 R/ or 800 photons $\text{cm}^{-2} \text{s}^{-1} \text{sr}^{-1} \text{\AA}^{-1}$. These spectra are dominated by the light of solar Lyman- α scattering off the interstellar hydrogen that is constantly flowing through the solar system. As *New Horizons* becomes more distant, this foreground component decreases, as is apparent from these observations that were made many months apart.

tion, but they do provide an estimate sufficient for our purposes. The data records consist of 191 $t_{\text{int}} = 10$ s integrations on the Pluto monitoring field taken from June 2012 to July 2014. Following calibration, for each field we find $R_L > 13.1$ sources and perform photometry on them using SOURCEEXTRACTOR in AUTO_MAG mode. We cross-identify the sources over images using their positions, and reject $R_L < 11.3$ sources as they saturate the detector in this integration time. Because the field is near the galactic plane, they suffer from source crowding, giving us a wide sampling of environments. Also, the position angle and pointing of the images shifts over the course of the observation epoch, so a particular

source is not always present in a given image. Figure 9 summarizes the photometry measurements for a selection of 20 relatively bright sources over the course of the observations.

To summarize the photometric performance of LORRI, we compute the mean absolute deviation of the flux measurements for each source. The results for the ensemble are summarized in Figure 8, scaled to a 6-hour observation period in $t_{\text{int}} = 10$ s integrations. We compare this to *Kepler's* “long integration” photometric accuracy (Vanderburg & Johnson 2014), and find LORRI is about an order of magnitude less accurate, which we would expect based on the differences in aperture size

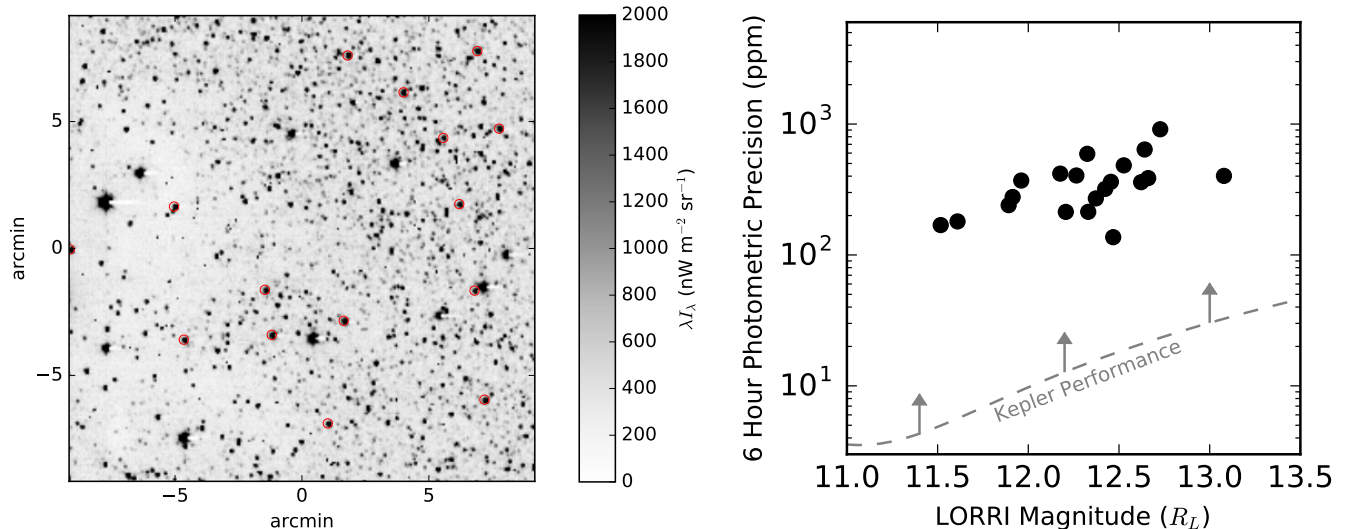


Figure 8. (Left Panel) An example image of the photometry stability field we study in this work. The image is calibrated as λI_λ . Stars selected for the photometry study described here are circled, and lie within $13.1 < R_L < 11.3$. Some of the stars used in the study do not fall into this image, but do fall in others in the set of observations. (Right Panel) An assessment of the photometric precision of LORRI based on 191 $t_{\text{int}} = 10\text{ s}$ observations acquired from summer 2012 to summer 2014. The points show the photometric precision measured from 20 stars in the field expressed as parts per million, referenced to 6 hours of 10 s observations. We compare this to the lower limit from the *Kepler* mission, which (in “long integration” mode) is about an order of magnitude more precise at these source fluxes. That difference in performance can be accounted by the different aperture size, integration time, and pointing control between these observations and *Kepler*’s.

and integration time. In fact, since the photometric accuracy of *Kepler* tends to have many low-precision outliers LORRI performs well in comparison, largely because the detectors for both instruments are similar. Importantly, we see no evidence for turn-on effects after ~ 1 year of hibernation, meaning that observations separated by long time intervals do not seem to suffer from transient effects related to power cycling.

4. STRAW MAN SURVEY OPERATIONS

Though the astrophysical science possible from *New Horizons* is compelling, there are practical considerations that limit the observations possible with the spacecraft. In this section, we discuss these limitations, their impacts on the science cases, and present a straw man operations scenario that would generate a rich and unique dataset. Properly designed, the new insights these observations would lead to are unlikely to be rivaled for the foreseeable future.

4.1. Attitude Control Considerations

Due to power considerations, *New Horizons* does not have a reaction wheel-based pointing system. Instead, hydrazine thrusters are used to provide pointing control. Attitude data from the star tracker and a laser-ring gyroscope system are input to a feedback loop to set the pointing within prescribed limits in both absolute astrometry and drift. In three-axis mode, a targeted posi-

tion can be found to within $1'.2$ (1σ), and active scans can be controlled to that location within a typical dead-band of $1'.7$. The achieved passive drift rate once an attitude has been achieved is $0''.5\text{ s}^{-1}$. Details of the attitude control system can be found in Rogers et al. (2006); Fountain et al. (2008).

In addition to the attitude control performance, the propellant required to point the spacecraft is a limiting factor to the observations performed during any extended mission. At this time, the predicted mass of propellant following the end of the KEM mission is 10 kg, as compared with about 40 kg remaining at the end of the primary Pluto flyby mission (Bushman 2017). As a benchmark, a change in *New Horizons*’ spin rate of 5 RPM (the change from the nominal spin rate to zero RPM for 3-axis control mode) requires approximately 0.125 kg of hydrazine (Fountain et al. 2008). Ultimately, the remaining propellant is likely to be the limiting factor in determining precisely which observations and science cases are possible in an extended mission for astrophysics.

4.2. Telemetry Considerations

Downlinking data from distant instruments has presented a challenge since the beginning of deep-space missions. As an example, the data acquired for the prime *New Horizons* Pluto fly-by mission required only one week to acquire, but over 16 months to telemeter back

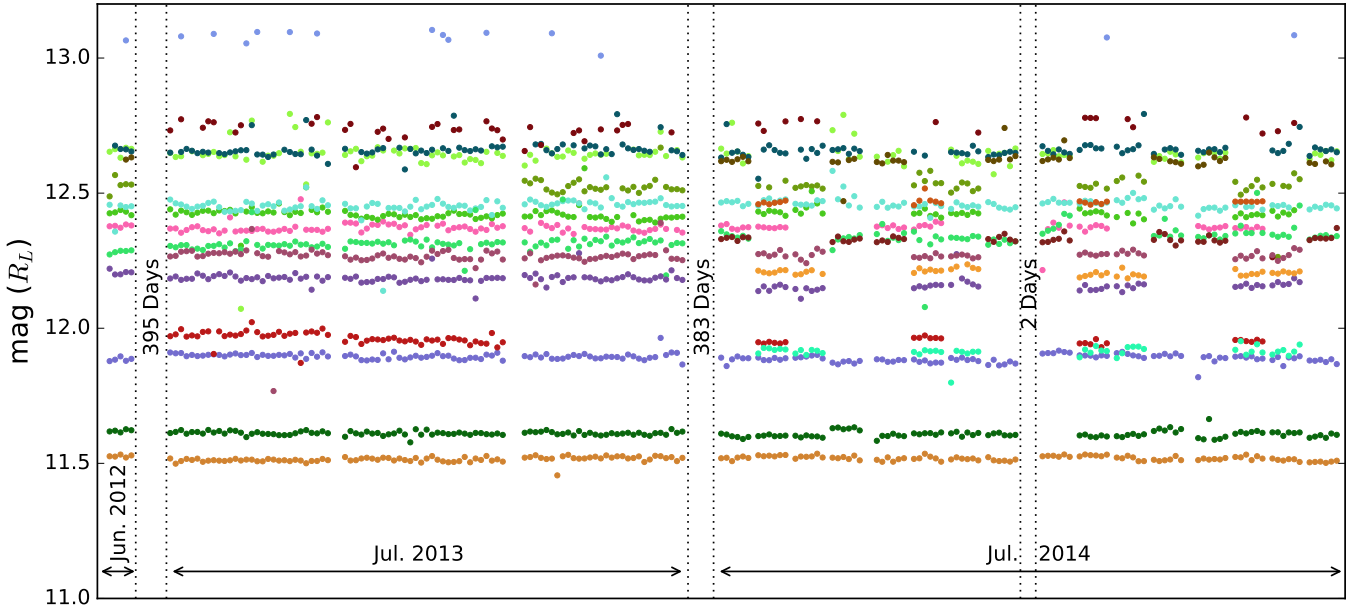


Figure 9. Measured fluxes of sources over three major observation epochs on the same field acquired between Jun. 2012 and Jul. 2014. The time axis has been compressed to aid visualization; gaps between points are roughly logarithmic, with the shortest corresponding to tens of seconds and the longest corresponding to hundreds of days. The largest temporal discontinuities are highlighted by vertical dashed lines. Because of the changing central position and position angle of the images with time, a given source may or may not be visible in a particular observation. The mean absolute deviation of these data referenced to a 6 hour baseline are shown in Figure 8. We find no evidence for effects related to waking the instrument after year-long hibernations, and find the stability of the detector is excellent over the period.

to Earth. The available bandwidth only decreases with time as the distance to *New Horizons* increases. In Figure 10, we show the achievable data rate from the beginning of the *New Horizons* mission until 2030, at which point the spacecraft will be some 80 AU from us (Fountain et al. 2008).

Assuming the proposed astronomical measurements do not occur until 2022 following the 2014 MU₆₉ extended mission, we expect a maximum data rate in three-axis pointing mode (*i.e.* the mode in which observations will be performed) to be ~ 900 bits per second (bps). If observational data were telemetered in spin-stabilized mode this increases to ~ 1.8 kbps. The per-frame size of the various *New Horizons* data products is given in Table 1, and typically measure in the ~ 10 Mb range. Assuming a 50% duty cycle, even at maximum telemetry speed this corresponds to only 80 Mb per day, which is approximately 40 mins of LORRI data, or 5 mins of MVIC/LEISA integrations.

4.3. Other Instrument Limitations

In addition to attitude control and telemetry, there are additional constraints on the instrument hardware to consider. The first of these is the maximum allowable integration time for the instruments, which was set to 30 s for LORRI (Cheng et al. 2008), 10 s for MVIC,

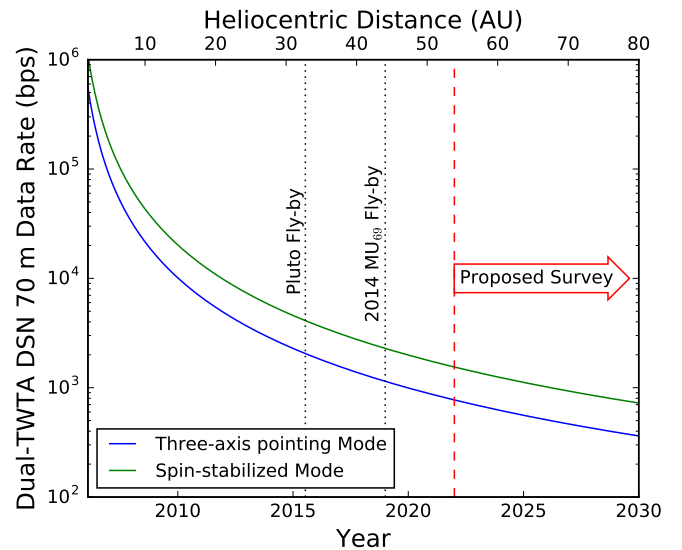


Figure 10. The data downlink rate from *New Horizons* versus time and heliocentric distance. The maximum achievable rate given in bits per second (bps) decreases as R_{\odot}^{-2} and depends on the attitude control mode of the spacecraft. In this calculation we assume the DSN 70m dish is used in Dual-TWTA mode (see Fountain et al. 2008 for details).

and 4 s for LEISA (Reuter et al. 2008) at launch. ALICE's maximum integration time of 600 s is less restric-

tive (Stern et al. 2008). For flux-limited observations, because of the low data downlink rate, it is desirable to increase the integration time to achieve equal sensitivity in fewer detector reads. However, because of *New Horizons*' relatively poor attitude control performance, longer integrations may suffer from image smearing as source images track along the detector. Given typical attitude drift rates, integrations lasting several minutes might offer an advantage. Such changes are feasible; the *New Horizons* team is in the process of increasing LORRI's maximum integration time to 60s (H. Weaver, private comm). Optimizing integration times requires a detailed trade study to understand the benefits and costs given the constrained attitude control, telemetry rate, and particulars of a science case, which we leave to future work.

A second consideration is the optical performance of the instruments. LORRI's rejection of off-axis light is relatively poor, such that viewing within a solar elongation angle of 90° results in scattered light in the image (Zemcov et al. 2017). Further, there are optical ghost paths between $0^\circ.2$ and $0^\circ.35$ from the optical axis, which leave out-of-focus images of the secondary mirror on the detector array (Cheng et al. 2010). In addition, LEISA suffers from a solar light leak with rays sensed by the detector coming from behind the instrument at the 10^{-7} level (Reuter et al. 2008). Though it is not difficult to work within these restrictions, some science cases (for example, imaging towards the inner solar system) are precluded. Other optical features that must be considered in the design of observations requiring high sensitivity and stability may also be present; this is another issue that requires detailed communication with the instrument teams to optimize.

4.4. Assessment of Science Cases

Given the instrument sensitivities and practical considerations discussed above, here we assess the feasibility of the different science cases presented in Section 2.

4.4.1. Measurement of EBL

Of the *New Horizons* instruments, the most sensitive instrument to diffuse emission is LORRI, which has the largest telescope aperture and widest bandpass. The expected IGL at LORRI's wavelength is $\sim 8 \text{ nW m}^{-2} \text{ sr}^{-1}$. As a result, if no pixel masking were required and only uncorrelated random noise were present, it should be possible to measure the IGL at $S/N \gtrsim 0.5$ in a single 30 s integration with LORRI. However, it is necessary to mask some fraction of pixels that contain bright stars, and the actual noise in the instrument is not ideal. As a result, the previous measurement (Zemcov et al. 2017) reached a statistical error of $7 \text{ nW m}^{-2} \text{ sr}^{-1}$ in 240 s of

integration time. To reach an uncertainty level comparable to the current uncertainty on IGL in a single field, some 400×30 s integrations would be required. In Table 2 we give estimates of the total number of integrations and total observation time required for this measurement (assuming no overheads), as well as an estimate of the time required to telemeter the data. Assuming a best telemetry rate of 1.8 kbps and 50% duty cycle, this data set would require 5 days to transmit to Earth. Though more time-consuming than the actual observations by a factor of 2,000, this is a relatively inexpensive measurement. Statistical sensitivity is not likely to limit this measurement as the CCD dark current stability, astrophysical foregrounds, and other effects would be relatively large at these low flux levels. The observation design would therefore rest on acquiring adequate knowledge of the system performance and foregrounds to be confident in the measurement.

With a pixel RMS of $> 4 \times 10^4 \text{ nW m}^{-2} \text{ sr}^{-1}$ in 10 s, MVIC would require $\sim 10^3$ integrations to reach a statistically significant EBL measurement, which in turn would require a few hours to execute. Information from all 5 MVIC channels would be telemetered at once, providing low resolution spectral information in the optical, which is an important addition to a LORRI measurement. However, the data telemetry for MVIC becomes a real consideration, with the transmission time for this data set estimated to be a significant fraction of a year. MVIC does have dark (*i.e.* non-illuminated) pixels to allow a measurement of the detector current in the absence of photons (Reuter et al. 2008), an important prerequisite to absolute photometric measurements (Matsuura et al. 2017).

Finally, LEISA would provide a unique measurement of the EBL, as it covers crucial infrared bands where observations of the emission from early galaxies are possible. LEISA's sensitivity is poor, and it would require at least two days equivalent observation time to execute observations that would yield a $\sim 3\sigma$ detection of the EBL per $R = 10$ band. However, we again encounter a situation where the data telemetry is time-consuming, largely due to the number of 4 s integrations required to achieve a useful surface brightness sensitivity. Though LEISA does not have built-in dark pixels, the instrument can be used in "Solar Illumination" mode where a small pick-off mirror assembly couples only $\sim 3,000$ pixels to external illumination (Reuter et al. 2008). A suitable choice of standard mode observations interspersed with Solar Illumination mode observations can offer close to real-time assessment of the dark current in the PICNIC detector array.

Table 2. Surface Brightness Sensitivity Targets and Requirements.

Instrument	Target Sensitivity ($\text{nW m}^{-2} \text{sr}^{-1}, 1\sigma$)	Number of Integrations Required ^a	Integration Time Required	Time to Telemeter ^b
LORRI	1	400	200 min	5 days
MVIC	2.5	1,500	240 min	330 days
LEISA (+10% SIM ^c)	5 (at $R = 10$)	25,000	27 hrs	315 days

^a Assumes maximum programmable integration time.

^b Assumes a data rate of 1.8 kbps and 50% data transmission duty cycle.

^c Assumes “Solar Illumination” mode (SIM) is used to monitor the dark current every 10 observations.

To prove isotropy of the measured EBL, it is necessary to observe several independent fields at high ecliptic and galactic latitudes to minimize foregrounds. Ground-based observations could then be used to help characterize the remaining local emission. For the LORRI observations this is not problematic, but is prohibitively expensive for the Ralph measurements. Clearly, the optimization of the number and position of fields to be observed, as well as an assessment of the systematic errors present in the instruments, should be the subject of detailed future work.

4.4.2. Ultraviolet Background Sensitivity

The nominal sensitivity of ALICE is ~ 1 R per pixel at $R = 133$ over a 1 Mpixel detector array in a 600 s integration. Averaging over pixels, we estimate a total background sensitivity of about 0.02 R/nm in this integration time, which corresponds to approximately 1,600 photons $\text{cm}^{-2} \text{s}^{-1} \text{sr}^{-1} \text{\AA}^{-1}$. Current estimates for the UV background place its surface brightness at < 100 photons $\text{cm}^{-2} \text{s}^{-1} \text{sr}^{-1} \text{\AA}^{-1}$, meaning that we would require 256 integrations to reach an interesting sensitivity limit (Henry et al. 2015). However, the UV background is faint compared to the galactic foregrounds, so ALICE is expected to yield interesting new information in only 30 integrations. Because ALICE observations are relatively inexpensive to telemeter, we would be able to both execute the observations and telemeter the resulting data in an equal amount of time. For 256 observations, we estimate 2 days of observation and 2 days of telemetry are required. This observation is inexpensive enough that many fields could be targeted on the sky, as long as propellant costs did not become problematic.

4.4.3. EKB Dust Observations

The primary regions of interest for IDP light scattering will be those centered on the ecliptic where the IDP density is highest, but also away from the galactic background, where DGL will contaminate the images. Though the very lowest levels of modeled IDP surface brightness would be too challenging to reach with LORRI, deep $< 1 \text{ nW m}^{-2} \text{sr}^{-1}$ sensitivities remain a real possibility, and would allow us to constrain

models for the composition and structure of the EKB. The example calculation of IDP brightness shown in Figure 4 assumes silicate grains; however, we can also input other dust grain compositions including ice mantle/silicate cores, carbonaceous, and organic compositions (e.g. Warren 1984; Jenniskens 1993; Quinten et al. 2002; Jäger et al. 2003). The observations would likely be performed as a function of solar elongation, and repeated over time as the sight line through the dust cloud changed to help deconvolve the structure profile. One interesting possibility to boost the signal is to measure the EKB analog to the Gegenschein, which is due to reflection of sunlight from dust in the directly anti-Solar direction that boosts the surface brightness of the local ZL signal by factors ~ 100 . Even upper limits to the EKB dust surface brightness would be unique and useful in this regard. We would estimate that ~ 10 positions at different solar elongations, observed every 5 AU in heliocentric radius, would make an excellent data set requiring only ~ 0.5 years to telemeter.

4.4.4. Exoplanet Transits

Exoplanet transits are typically studied in relatively bright star systems, and require photometric accuracy better than 1:1000 over ~ 1 hour timescales. For a $V = 8$ star, we would require a 1σ photometric accuracy of $\delta V = 15.5$ to detect the presence of the planet around e.g. HD209458, which is significantly above LORRI’s $t_{\text{int}} = 30$ s sensitivity. This bodes well for the use of LORRI in observing transits.

Due to propellant use, it would be far too expensive to operate LORRI in a constant-monitoring mode as was done with e.g. *Kepler*. A more efficient use of the finite resources would be to target known transiting systems, and to use the remarkably stable detector to search for faint structures around planets. Both the transit timing and transit duration methods require precise measurements of a planet’s light curve over many transits to build up a model of the moon’s orbit. This requires many transit measurements separated by possibly years from an instrument that is known to be stable. LORRI could be used to study known transiting systems with a cadence that observes each target during a number

of transits over a timescale given by the length of the mission. The quiet environment and diagnostic information about the detector would be very useful in ensuring instrument stability of this time. LORRI could also be used to measure the orbit sampling effect, which requires $\sim 1 : 10^4$ photometric stability, and (again) multiple measurement of a transiting system to sample different phases in the moon’s orbit. The example given above is within the 1σ statistical uncertainty for relatively bright, local systems. In fact, all three moon detection methods rely on well-understood and low-error light curves, which *New Horizons* is in a unique position to generate.

In terms of operations, the data requirement of, for example, a 30 s observation every 5 minutes for 2 hours would generate only 24 frames for telemetry. The requirement of pointing stability would be more problematic, as would the active pointing required to keep the source in the same pixels over time, since this requires active use of propellant. This expenditure would have to be traded in the context of the larger mission goals and observations.

4.4.5. Microlensing

Microlensing events can magnify the source star by up to several magnitudes over the course of events lasting between ~ 1 day to several months. Single-lens events can be detected with a relatively low cadence (once every 0.5-3 days) survey. However, binary events, both stellar and planetary which comprise $\sim 10\%$ of the total, are characterized by short-lived (\sim hours – days) lightcurve anomalies which must be sufficiently well sampled as to constrain the model. Typical observations aim for a photometric precision of <0.01 mag, and a cadence of at least 4 hours $^{-1}$. We consider the practical implications of several possible observing strategies.

LORRI’s wide field of view suggests a survey strategy where *New Horizons* would repeatedly image the region of highest microlensing rate, over the course of >2 months. The overall length of the observations is determined by the need to measure the lensing lightcurve both over the peak of the event and at baseline (unlensed) in order to properly constrain the event magnification and timescale. Surveying the full $\sim 3^\circ.3 \times 3^\circ.3$ central Bulge region would require a 11×11 mosaic of LORRI images. Although in principle it could achieve a cadence of ~ 4 hrs, this strategy would be prohibitively expensive on propellant. Furthermore, it would accumulate data far in excess of the downlink capacity – ~ 11.9 GB/day (noting that Bulge observations could not be binned in order to preserve spatial resolution). Surveying 4 LORRI field pointings once a day (or con-

versely, 1 field every 6 hrs) has a more practical data rate of 67.2 MB day $^{-1}$. The wider footprint would ensure more events are detected (~ 22 year $^{-1}$ vs. ~ 5 year $^{-1}$) while a single pointing would conserve propellant.

A second possible strategy would take advantage of *New Horizons*’ unique position to act as “early warning system”. As noted above, some fraction of events observed by *New Horizons* may subsequently be observed from Earth in separate lensing events after a delay of over 1 yr. Were the spacecraft to undertake a very wide angle, but low (~ 1 -3 day) cadence survey of a wide region, there would be plenty of time to downlink the data and discover events which could then be intensively followed-up from Earth and near-Earth missions. LORRI could survey a 4×4 grid of pointings, $\sim 1^\circ.16 \times 1^\circ.16$ each, once every 3 days with a data rate of 89.6 MB day $^{-1}$.

The final option would be the converse: to use *New Horizons* to follow-up selected events discovered from Earth and/or by *WFIRST*. Events observed from both Earth and *WFIRST* will already have constraints on the lens-source relative trajectory, allowing more stringent target selection, and many will already be known to have planetary or binary signatures. In this way, *New Horizons* could act as a “force multiplier” for those surveys, to search for other planetary or stellar companions in the same systems thanks to its distinct line of sight to the event. This strategy would require higher cadence observations (ideally <1 hr) but over a shorter period during the peak of the event, with lower cadence (every ~ 3 days) observations taken before and after the peak to measure the event magnification.

4.4.6. Transient Follow-Up

LORRI certainly has the point source sensitivity to reach the flux of some transient sources, and is stable over long time periods. Measurement of transient events would require a “fast track” observation upload scheme. It is likely that at least several days would pass between the detection of an event and a *New Horizons* observation taking place, and data would not necessarily be telemetered immediately. Further, these measurements would only be useful for the period when *New Horizons* is near the sun as viewed from the Earth and observation from the ground is impossible. It would make sense to optimize the *New Horizons* observation epochs to coincide with these periods, so that the instrument would already be in a mode to execute astrophysical observations. This requirement may not be compatible with communication using the high-gain antenna. As a result of all of these extra requirements, the use of *New*

Horizons for transient measurements remains somewhat speculative at this point.

4.5. A Straw Man Observational Campaign

In designing an observational campaign, there are three major factors to consider: (i) the time required to telemeter the data back to Earth, and the storage capacity and reliability of the on-board data volumes; (ii) the need to expend fuel for observations requiring active pointing control; and (iii) optical and communications restrictions on the attitude of the spacecraft.

As shown in Table 2, the time to telemeter the data can easily grow to be prohibitive. The most cost-efficient instrument in terms of sensitivity per data volume is LORRI, and we assume that most of the observations would be performed with it. Even so, the data storage considerations impose a survey design similar to the *New Horizons*' planetary encounters, where an observation campaign is pre-programmed and executed contiguously, and then later telemetered to Earth while the spacecraft is in spin-stabilized mode. This scheme takes advantage of the downlink rate boost of spin-stabilized mode. Based on purely data telemetry considerations, we therefore propose a scheme where observations are performed roughly annually in a short burst, and then telemetered during a cruise phase. This pattern could be repeated for many years, and would ultimately be limited by the fuel required to maneuver the spacecraft.

The attitude control system likely limits the lifetime of the mission. In order to conserve the resource, observations that would not require active pointing control, or at least could be performed with periodic pointing correction, would be preferable. Assuming the nominal post-acquisition drift rate of $0''.5 \text{ sec}^{-1}$, a target centered on the LORRI detector array would drift off the field of view in > 17 minutes. This sets a natural cadence for attitude correction during measurements of point sources that minimizes fuel consumption. For deep observations of diffuse surface brightness, and even more conservative viewing mode would be to point the telescope on-target, and then let it drift for some specified time before re-pointing. For observations of emission that varies smoothly over sub-degree scales (for example, EBL, DGL, or IPD), the spacecraft could wander for 1 hour, at which time the center of the field of view would have drifted by $0^\circ.5$. Point source emission could easily be masked following the post-facto image registration, and foreground emission requiring image-space correlation could just use the reconstructed pointing of each image separately. The most challenging measurements are those requiring photometric precision, where drift causes a source to wander between pixels that have

different relative photoresponse. These observations are likely to require tighter attitude control than studies of diffuse brightness. However, if controlled, in this work we have shown that LORRI can perform adequately to allow unique observations of both exoplanet transits and microlensing.

The third consideration in our survey design are attitude constraints due to the instruments, communications, or other features of the spacecraft. One obvious constraint is for the imaging instruments to have a solar elongation $> 90^\circ$ at all times during an observation, which constrains the field of regard to 2π sr away from the Sun, which are likely to be frozen in celestial coordinates for the duration of the mission. There are almost certainly additional constraints for the high-gain antenna and other systems, and for keeping the solar illumination of the spacecraft roughly constant to minimize thermal disturbances.

All of these constraints considered, *New Horizons* is still capable of generating a rich and unique data set for astrophysical science. For the EBL science case, we would measure 5–10 independent fields with LORRI to $\pm 1 \text{ nW m}^{-2} \text{ sr}^{-1}$ to show isotropy in the signal, and at least one field to $\pm 3 \text{ nW m}^{-2} \text{ sr}^{-1}$ error with MVIC and $\pm 4 \text{ nW m}^{-2} \text{ sr}^{-1}$ error with LEISA. These measurements would require a large number of integrations added together, likely acquired over different epochs.

A measurement of the UV background with ALICE is quite tractable, and requires only of order days of integration and telemetry time to achieve interesting sensitivities that cannot be reached from vantage points near the Earth. The scientific goals of our proposed ALICE observations are served well by any and all observations of any regions of the sky. Particularly valuable will be comparison of ALICE spectra obtained while pointed toward regions at high galactic latitudes compared against the same at low galactic latitudes (where starlight scattered from dust is expected to dominate the spectra, demonstrating instrumental capability). Valuable data will be obtained on any target that is observed in pointed mode, and the pointing stability can drift considerably without harm to the value of the data obtained. To conserve propellant and aid in cross-correlation studies, it is likely that the UV measurements would be performed concurrently with and on the same fields as the EBL measurements. Obviously, it would be necessary to develop a detailed observation plan that would optimize the observation strategy.

For the EKB dust measurement, we would measure ~ 10 fields placed at different ecliptic latitudes in each epoch of a multi-year mission. Because the EKB dust is spatially smooth, these observations would not require

tight pointing control. Measuring to $\pm 1 \text{ nW m}^{-2} \text{ sr}^{-1}$ error with LORRI in each epoch would allow a detailed probe of the structure of the EKB. Spectral information from MVIC and LEISA is likely too expensive to be considered, but the EBL measurements may permit interesting constraints on the longer wavelength behavior of the EKB dust emission. It is likely these fields and the extragalactic background fields would be designed in a coordinated fashion, since the observational requirements are very similar.

In our envisioned survey we would also observe a subset of known transiting systems (so that the exo-ecliptic plane is along the line of sight) around bright stars to search for faint transits. The subset can be selected based on prioritization of targets for future coronagraphic imaging with *WFIRST*. Searches for extrasolar moons can be performed over a several day spans as the transit time of the parent planet is known from existing observations. These observations require pointing on a particular target for long periods of time with observations at a relatively fast cadence (~ 10 per hour), so would be expensive in terms of propellant. Assuming a 2-day measurement with a 5-minute cadence of 30 s LORRI observations, we would require 576 frames to be telemetered. Potentially, $\gtrsim 10$ such systems could be surveyed in a year.

Traditional exoplanet microlensing measurements require close to constant monitoring of fields in the galactic bulge region to increase the number of possible targets. A microlensing survey based on this design would thus require fairly constant sampling of a single target field for as long a baseline as possible, and active pointing correction to keep the field of view on target. Here, we envision a different approach. An Earth-based microlensing survey monitoring a known field could have a real-time event pipeline that triggers on suspected star-star lensing events. During *New Horizons* observation campaigns, these triggers could be passed to the science team and programmed into the queue with priority. The ~ 10 day duration of these events gives ample time to design and upload an observation into the queue. The light curve of the source would be monitored for several days, and short-duration microlensing events indicative of exoplanets could be sought.

Science cases that require point source photometry would benefit from windowing the image to a region around the target of interest, as this would significantly reduce the telemetry bandwidth requirement. At the other extreme, on-board co-addition of images could allow an increase in the signal to noise ratio of static sources of emission. Both algorithms would have to take into account the drift of the images over time, unless

the spacecraft attitude can be controlled to the necessary level over time. Finally, to maximize the available fuel resources, observations would need to be designed to minimize slew distances on the sky. Since observations are planned well in advance (except for microlensing events), this is not a prohibitive requirement. Following a ~ 1 week long observation campaign each year, *New Horizons* would go into spin-stabilized mode and begin transmitting the data to Earth.

4.6. *The Possibility of Science Observations During Spin-Stabilized Operations*

Given the limited propellant budget for pointed observations, one possibility of interest is to perform astrophysical observations in some form of the spin-stabilized operation. This would provide the benefit of increasing the data telemetry rate while allowing different parts of the sky to be surveyed by the instruments. The primary drawback of this scheme is related to the detectors; all of the detectors on the *New Horizons* instrument suite suitable for astrophysical observations are of the charge integrating type, which usually require stable pointing over the course of an integration to provide clean images of the sky. The cost of having *New Horizons* spin during observations is that the astrophysical signal would be smeared over multiple pixels, thereby confusing image analysis and, in the limit of read-noise limited measurements, decreasing the total signal to noise ratio on the source. For a purely isotropic signal, or one that is not spatially structured on the angular scale of the spin smear, this is not problematic. However, most of the science cases discussed here require spatial resolution either to monitor a point-like source, or to remove it through masking. As a result, allowing the spacecraft to spin could be problematic.

In *New Horizons*' standard spin-stabilized mode the spacecraft is spinning around the high-gain antenna's boresight at 5 RPM, which corresponds to $30^\circ \text{ minute}^{-1}$. This is clearly prohibitively fast, as it means (for example) that LORRI's field of view is moving one full array width every 0.6 s. Even in unreasonably short integration times, images of stars would be smeared. As a conservative estimate for the preferred spin rate, we impose the requirement that, over a full 30 s integration, the LORRI image can shift by 0.5 pixels, or 2 arcsec. This corresponds to a spin rate of 3.1×10^{-6} RPM, which is clearly a different engineering regime than the current spin-stabilized mode. Due to their larger pixels and shorter integration times, the other instruments could accept relatively faster spin rates, though still within an order of magnitude of the LORRI requirement. Faster spin rates may also be acceptable, with a concomitant

loss in scientific capability. This kind of observation may be enabling for EBL science with MVIC and LEISA, where the required integration times and data volumes are probably prohibitive in pointed mode, but if the observations can be spread over many months they become more tractable.

We conclude that, though it may be technically challenging to implement, it is worth studying the possibility of a spin-stabilized mode with a very slow spin rate. Observing in this mode would not require any propellant, would increase the data telemetry rate, and would allow maps of large areas of sky to be constructed. Some of the science cases, particularly those related to diffuse emission, could potentially benefit from such an observation strategy.

5. CONCLUSIONS

With a fully functioning *New Horizons* beyond the orbit of Pluto, the astrophysical and planetary communities have a rare opportunity to perform unique science with an instrumentation suite capable of deep and precise observation of the cosmos. In this paper we have motivated the broad scientific fields such observations can address, as well as studied the performance of the instruments and discussed the various limitations and considerations a future survey with *New Horizons* would have to address. We find that *New Horizons* is well suited to astrophysical observation, and that a carefully

designed survey optimizing the expenditure of propellant and telemetry bandwidth while minimizing spacecraft operational risk could provide interesting new insights in astrophysics. Some data of astrophysical interest is already available in the archive, and the analysis of these is ongoing. Insights from these will help us design better observations. Going forward, we suggest a study of the detailed feasibility of astrophysical observations with *New Horizons* combining the *New Horizons* instrument and engineering teams with astrophysical experts in the various scientific fields discussed here. This will permit an accurate assessment of the current capabilities of the instruments and spacecraft and a detailed observation plan to be formulated.

We would like to thank the *New Horizons* science and instrument teams for their decades of dedicated effort designing, building and flying such a complex mission, and in particular H. Weaver for his patience in answering our largely impenetrable queries. We would also like to thank B. Crill for his insightful comments that helped improve the work.

The *New Horizons* cruise phase data sets used in this work were obtained from the Planetary Data System (PDS). Support for IA was provided by NASA through the Einstein Fellowship Program, grant PF6-170148. A.R.P. was supported by the NASA Planetary Atmospheres program, grant #NNX13AG55G.

REFERENCES

- Abbott, B. P., Abbott, R., Abbott, T. D., et al. 2017a, *Physical Review Letters*, 119, 161101, doi: [10.1103/PhysRevLett.119.161101](https://doi.org/10.1103/PhysRevLett.119.161101)
- . 2017b, *ApJL*, 848, L12, doi: [10.3847/2041-8213/aa91c9](https://doi.org/10.3847/2041-8213/aa91c9)
- . 2017c, *Nature*, 551, 85, doi: [10.1038/nature24471](https://doi.org/10.1038/nature24471)
- Altobelli, N., Dikarev, V., Kempf, S., et al. 2007, *J. Geophys. Res.*, 112
- Arcavi, I., McCully, C., Hosseinzadeh, G., et al. 2017a, *ApJL*, 848, L33, doi: [10.3847/2041-8213/aa910f](https://doi.org/10.3847/2041-8213/aa910f)
- Arcavi, I., Hosseinzadeh, G., Howell, D. A., et al. 2017b, *Nature*, 551, 64, doi: [10.1038/nature24291](https://doi.org/10.1038/nature24291)
- Bernstein, R. A. 2007, *ApJ*, 666, 663, doi: [10.1086/519824](https://doi.org/10.1086/519824)
- Bock, J., Beichman, C., Cooray, A., et al. 2012, *SPIE Newsroom*, doi: [10.1117/2.1201202.004144](https://doi.org/10.1117/2.1201202.004144)
- Bock, J., Sullivan, I., Arai, T., et al. 2013, *ApJS*, 207, 32, doi: [10.1088/0067-0049/207/2/32](https://doi.org/10.1088/0067-0049/207/2/32)
- Bohlin, R. C. 2014, *AJ*, 147, 127, doi: [10.1088/0004-6256/147/6/127](https://doi.org/10.1088/0004-6256/147/6/127)
- Borucki, W. J., Koch, D., Basri, G., et al. 2010, *Science*, 327, 977, doi: [10.1126/science.1185402](https://doi.org/10.1126/science.1185402)
- Bowyer, S. 1991, *ARA&A*, 29, 59, doi: [10.1146/annurev.aa.29.090191.000423](https://doi.org/10.1146/annurev.aa.29.090191.000423)
- Boyajian, T. S., LaCourse, D. M., Rappaport, S. A., et al. 2016, *MNRAS*, 457, 3988, doi: [10.1093/mnras/stw218](https://doi.org/10.1093/mnras/stw218)
- Broadfoot, A. L., Sandel, B. R., Shemansky, D. E., et al. 1977, *SSRv*, 21, 183, doi: [10.1007/BF00200850](https://doi.org/10.1007/BF00200850)
- Buchalter, A., & Kamionkowski, M. 1997, *ApJ*, 482, 782, doi: [10.1086/304163](https://doi.org/10.1086/304163)
- Burns, J. A., Lamy, P. L., & Soter, S. 1979, *Icarus*, 40, 1
- Bushman, S. S. 2017, Performance of the New Horizons Propulsion System through the Pluto Encounter (American Institute of Aeronautics and Astronautics). <https://doi.org/10.2514/6.2017-4746>
- Caldwell, D. A., Kolodziejczak, J. J., Van Cleve, J. E., et al. 2010, *ApJL*, 713, L92, doi: [10.1088/2041-8205/713/2/L92](https://doi.org/10.1088/2041-8205/713/2/L92)
- Cambrésy, L., Reach, W. T., Beichman, C. A., & Jarrett, T. H. 2001, *ApJ*, 555, 563, doi: [10.1086/321470](https://doi.org/10.1086/321470)
- Chary, R.-R., & Pope, A. 2010, arXiv, 1003

- Cheng, A. F., Conard, S. J., Weaver, H. A., Morgan, F., & Noble, M. 2010, in Proc. SPIE, Vol. 7731, Space Telescopes and Instrumentation 2010: Optical, Infrared, and Millimeter Wave, 77311A
- Cheng, A. F., Weaver, H. A., Conard, S. J., et al. 2008, SSRv, 140, 189, doi: [10.1007/s11214-007-9271-6](https://doi.org/10.1007/s11214-007-9271-6)
- Christon, S. P., Hamilton, D. C., Plane, J. M. C., et al. 2015, J. Geophys. Res.: Space Physics, 120, 2720
- Conard, S. J., Azad, F., Boldt, J. D., et al. 2005, in Proc. SPIE (2005), Vol. 5906, *Astrobiology and Planetary Missions* (Eds. Hoover, R. B. et al.) 407-420, ed. R. B. Hoover, G. V. Levin, A. Y. Rozanov, & G. R. Gladstone, 407-420
- Cooray, A. 2016, Royal Society Open Science, 3, 150555, doi: [10.1098/rsos.150555](https://doi.org/10.1098/rsos.150555)
- Cooray, A., Bock, J. J., Keatin, B., Lange, A. E., & Matsumoto, T. 2004, ApJ, 606, 611, doi: [10.1086/383137](https://doi.org/10.1086/383137)
- Cooray, A., Amblard, A., Beichman, C., et al. 2009
- Cuzzi, J. N., & Estrada, P. R. 1998, Icarus, 132, 1
- Dixon, W. V. D., Sankrit, R., & Otte, B. 2006, ApJ, 647, 328, doi: [10.1086/505168](https://doi.org/10.1086/505168)
- Dong, S., Udalski, A., Gould, A., et al. 2007, ApJ, 664, 862, doi: [10.1086/518536](https://doi.org/10.1086/518536)
- Drout, M. R., Piro, A. L., Shappee, B. J., et al. 2017, ArXiv e-prints. <https://arxiv.org/abs/1710.05443>
- Durisen, R. H., Cramer, N. L., Murphy, B. W., et al. 1989, Icarus, 80, 136
- Edelstein, J., Bowyer, S., & Lampton, M. 2000, ApJ, 539, 187, doi: [10.1086/309192](https://doi.org/10.1086/309192)
- Estrada, P. R., Durisen, R. H., Cuzzi, J. N., & Morgan, D. A. 2015, Icarus, 252, 415
- Feuchtgruber, H., Lellouch, E., de Graauw, T., et al. 1997, Nature, 389, 159
- Fountain, G. H., Kusnierkiewicz, D. Y., Hersman, C. B., et al. 2008, SSRv, 140, 23, doi: [10.1007/s11214-008-9374-8](https://doi.org/10.1007/s11214-008-9374-8)
- Frankland, V. L., James, A. D., Carrillo-Sánchez, J. D., et al. 2016, Icarus, 278, 88
- Gehrels, N., Cannizzo, J. K., Kanner, J., et al. 2016, ApJ, 820, 136, doi: [10.3847/0004-637X/820/2/136](https://doi.org/10.3847/0004-637X/820/2/136)
- Gladstone, G. R., Stern, S. A., & Pryor, W. R. 2013, New Horizons Cruise Observations of Lyman- α Emissions from the Interplanetary Medium, ed. E. Quémerais, M. Snow, & R.-M. Bonnet, 177
- Gong, Y., Cooray, A., Mitchell-Wynne, K., et al. 2016, ApJ, 825, 104, doi: [10.3847/0004-637X/825/2/104](https://doi.org/10.3847/0004-637X/825/2/104)
- Gordon, K. D., Witt, A. N., & Friedmann, B. C. 1998, ApJ, 498, 522, doi: [10.1086/305571](https://doi.org/10.1086/305571)
- Gorjian, V., Wright, E. L., & Chary, R. R. 2000, ApJ, 536, 550, doi: [10.1086/308974](https://doi.org/10.1086/308974)
- Gould, A. 1992, ApJ, 392, 442, doi: [10.1086/171443](https://doi.org/10.1086/171443)
- Gould, A., Udalski, A., Monard, B., et al. 2009, ApJL, 698, L147, doi: [10.1088/0004-637X/698/2/L147](https://doi.org/10.1088/0004-637X/698/2/L147)
- Grigorieva, A., Thébault, P., Artymowicz, P., & Brandeker, A. 2007, Astron. Astrophys., 475, 755
- Grün, E., et al. 1995a, Planet. Space Sci., 43, 971
- . 1995b, Planet. Space Sci., 43, 953
- Gurnett, D. A., Ansher, J. A., Kurth, W. S., & Granroth, L. J. 1997, Geophys. Res. Lett., 24, 3125
- Gustafson, B. A. S. 1994, Annu. Rev. Earth Planet. Sci., 22, 553
- Hahn, J. M., Zook, H. A., Cooper, B., & Sunkara, B. 2002, Icarus, 158, 360
- Hamden, E. T., Schiminovich, D., & Seibert, M. 2013, ApJ, 779, 180, doi: [10.1088/0004-637X/779/2/180](https://doi.org/10.1088/0004-637X/779/2/180)
- Han, D., Poppe, A. R., Piquette, M., Grün, E., & Horányi, M. 2011, Geophys. Res. Lett., 38
- Hanner, M. S., Weinberg, J. L., DeShields, II, L. M., Green, B. A., & Toller, G. N. 1974, J. Geophys. Res., 79, 3671, doi: [10.1029/JA079i025p03671](https://doi.org/10.1029/JA079i025p03671)
- Hauser, M. G., & Dwek, E. 2001, ARA&A, 39, 249, doi: [10.1146/annurev.astro.39.1.249](https://doi.org/10.1146/annurev.astro.39.1.249)
- Hedman, M. M., Murray, C. D., Cooper, N. J., et al. 2009, Icarus, 199, 378
- Heller, R. 2014, ApJ, 787, 14, doi: [10.1088/0004-637X/787/1/14](https://doi.org/10.1088/0004-637X/787/1/14)
- . 2017, ArXiv e-prints. <https://arxiv.org/abs/1701.04706>
- Heller, R., Hippke, M., & Jackson, B. 2016a, ApJ, 820, 88, doi: [10.3847/0004-637X/820/2/88](https://doi.org/10.3847/0004-637X/820/2/88)
- Heller, R., Hippke, M., Placek, B., Angerhausen, D., & Agol, E. 2016b, A&A, 591, A67, doi: [10.1051/0004-6361/201628573](https://doi.org/10.1051/0004-6361/201628573)
- Henry, R. C. 1991, ARA&A, 29, 89, doi: [10.1146/annurev.aa.29.090191.000513](https://doi.org/10.1146/annurev.aa.29.090191.000513)
- Henry, R. C., Murthy, J., Overduin, J., & Tyler, J. 2015, ApJ, 798, 14, doi: [10.1088/0004-637X/798/1/14](https://doi.org/10.1088/0004-637X/798/1/14)
- H.E.S.S. Collaboration, Abramowski, A., Acero, F., et al. 2013, A&A, 550, A4, doi: [10.1051/0004-6361/201220355](https://doi.org/10.1051/0004-6361/201220355)
- Holberg, J. B. 1986, ApJ, 311, 969, doi: [10.1086/164834](https://doi.org/10.1086/164834)
- Holberg, J. B., & Barber, H. B. 1985, ApJ, 292, 16, doi: [10.1086/163128](https://doi.org/10.1086/163128)
- Horányi, M., Hoxie, V., James, D., et al. 2008, SSRv, 140, 387, doi: [10.1007/s11214-007-9250-y](https://doi.org/10.1007/s11214-007-9250-y)
- Howett, C. J. A., Parker, A. H., Olkin, C. B., et al. 2017, Icarus, 287, 140, doi: [10.1016/j.icarus.2016.12.007](https://doi.org/10.1016/j.icarus.2016.12.007)
- Humes, D. H. 1980, J. Geophys. Res., 85, 5841
- Ipatov, S. I., Kutyrev, A. S., Madsen, G. J., et al. 2008, Icarus, 194, 769
- Jäger, C., Dorschner, J., Mutschke, H., Posch, T., & Henning, T. 2003, Astron. Astrophys., 408, 193

- Jenniskens, P. 1993, *Astron. Astrophys.*, 274, 653
- Keenan, R. C., Barger, A. J., Cowie, L. L., & Wang, W.-H. 2010, *ApJ*, 723, 40, doi: [10.1088/0004-637X/723/1/40](https://doi.org/10.1088/0004-637X/723/1/40)
- Kelley, M. S., Fernández, Y. R., Licandro, J., et al. 2013, *Icarus*, 225, 475
- Kipping, D. M., Fossey, S. J., Campanella, G., Schneider, J., & Tinetti, G. 2010, in *Astronomical Society of the Pacific Conference Series*, Vol. 430, *Pathways Towards Habitable Planets*, ed. V. Coudé du Foresto, D. M. Gelino, & I. Ribas, 139
- Leinert, C., Bowyer, S., Haikala, L. K., et al. 1998, *A&AS*, 127, 1, doi: [10.1051/aas:1998105](https://doi.org/10.1051/aas:1998105)
- Levenson, L. R., Wright, E. L., & Johnson, B. D. 2007, *ApJ*, 666, 34, doi: [10.1086/520112](https://doi.org/10.1086/520112)
- Liou, J.-C., Zook, H. A., & Dermott, S. F. 1996, *Icarus*, 124, 429
- Liou, J.-C., Zook, H. A., & Jackson, A. A. 1995, *Icarus*, 116, 186
- Madau, P., & Pozzetti, L. 2000, *MNRAS*, 312, L9, doi: [10.1046/j.1365-8711.2000.03268.x](https://doi.org/10.1046/j.1365-8711.2000.03268.x)
- Mather, J. C., & Beichman, C. A. 1996, in *American Institute of Physics Conference Series*, Vol. 348, *American Institute of Physics Conference Series*, ed. E. Dwek, 271–277
- Matsumoto, T., Matsuura, S., Murakami, H., et al. 2005, *ApJ*, 626, 31, doi: [10.1086/429383](https://doi.org/10.1086/429383)
- Matsuoka, Y., Ienaka, N., Kawara, K., & Oyabu, S. 2011, *ApJ*, 736, 119, doi: [10.1088/0004-637X/736/2/119](https://doi.org/10.1088/0004-637X/736/2/119)
- Matsuura, S., Yano, H., Yonetoku, D., et al. 2014, *TRANSACTIONS OF THE JAPAN SOCIETY FOR AERONAUTICAL AND SPACE SCIENCES, AEROSPACE TECHNOLOGY JAPAN*, 12, Tr.1
- Matsuura, S., Arai, T., Bock, J. J., et al. 2017, *ApJ*, 839, 7, doi: [10.3847/1538-4357/aa6843](https://doi.org/10.3847/1538-4357/aa6843)
- Mattila, K. 2003, *ApJ*, 591, 119, doi: [10.1086/375182](https://doi.org/10.1086/375182)
- . 2006, *MNRAS*, 372, 1253, doi: [10.1111/j.1365-2966.2006.10934.x](https://doi.org/10.1111/j.1365-2966.2006.10934.x)
- Mattila, K., Lehtinen, K., Väisänen, P., von Appen-Schnur, G., & Leinert, C. 2012, in *IAU Symposium*, Vol. 284, *The Spectral Energy Distribution of Galaxies - SED 2011* (Eds. Tuffs, R. J. and Popescu, C. C.) 429–436, ed. R. J. Tuffs & C. C. Popescu, 429–436
- Mattila, K., Väisänen, P., Lehtinen, K., von Appen-Schnur, G., & Leinert, C. 2017, *MNRAS*, 470, 2152, doi: [10.1093/mnras/stx1296](https://doi.org/10.1093/mnras/stx1296)
- Morgan, F., Conard, S. J., Weaver, H. A., et al. 2005, in *Proc. SPIE*, Vol. 5906, *Astrobiology and Planetary Missions* (Eds. Hoover, R. B. et al.) 421–432, ed. R. B. Hoover, G. V. Levin, A. Y. Rozanov, & G. R. Gladstone, 421–432
- Moses, J. I. 1992, *Icarus*, 99, 368
- Moses, J. I., Lellouch, E., Bézard, B., et al. 2000, *Icarus*, 145, 166
- Moses, J. I., & Poppe, A. R. 2017, *Icarus*, *in review*
- Mroz, P., Ryu, Y.-H., Skowron, J., et al. 2017, *ArXiv e-prints*. <https://arxiv.org/abs/1712.01042>
- Muraki, Y., Han, C., Bennett, D. P., et al. 2011, *ApJ*, 741, 22, doi: [10.1088/0004-637X/741/1/22](https://doi.org/10.1088/0004-637X/741/1/22)
- Murthy, J. 2009, *Ap&SS*, 320, 21, doi: [10.1007/s10509-008-9855-y](https://doi.org/10.1007/s10509-008-9855-y)
- . 2016, *MNRAS*, 459, 1710, doi: [10.1093/mnras/stw755](https://doi.org/10.1093/mnras/stw755)
- Murthy, J., Hall, D., Earl, M., Henry, R. C., & Holberg, J. B. 1999, *ApJ*, 522, 904, doi: [10.1086/307652](https://doi.org/10.1086/307652)
- Murthy, J., Henry, R. C., & Holberg, J. B. 1991, *ApJ*, 383, 198, doi: [10.1086/170776](https://doi.org/10.1086/170776)
- Murthy, J., Henry, R. C., Shelton, R. L., & Holberg, J. B. 2001, *ApJL*, 557, L47, doi: [10.1086/323041](https://doi.org/10.1086/323041)
- Murthy, J., Im, M., Henry, R. C., & Holberg, J. B. 1993, *ApJ*, 419, 739, doi: [10.1086/173524](https://doi.org/10.1086/173524)
- Nesvorný, D., Vokrouhlický, D., Pokorný, P., & Janches, D. 2011, *Astrophys. J.*, 743
- Nissanke, S., Kasliwal, M., & Georgieva, A. 2013, *ApJ*, 767, 124, doi: [10.1088/0004-637X/767/2/124](https://doi.org/10.1088/0004-637X/767/2/124)
- Noble, M. W., Conard, S. J., Weaver, H. A., Hayes, J. R., & Cheng, A. F. 2009, in *Proc. SPIE*, Vol. 7441, *Instruments and Methods for Astrobiology and Planetary Missions XII*, 74410Y
- Olkin, C. B., Reuter, D., Lunsford, A., Binzel, R. P., & Stern, S. A. 2006, in *Bulletin of the American Astronomical Society*, Vol. 38, *AAS/Division for Planetary Sciences Meeting Abstracts #38*, 597
- Pian, E., D’Avanzo, P., Benetti, S., et al. 2017, *Nature*, 551, 67, doi: [10.1038/nature24298](https://doi.org/10.1038/nature24298)
- Poleski, R. 2016, *MNRAS*, 455, 3656, doi: [10.1093/mnras/stv2569](https://doi.org/10.1093/mnras/stv2569)
- Poppe, A., & Horányi, M. 2011, *Planet. Space Sci.*, 59, 1647
- Poppe, A., James, D., Jacobsmeyer, B., & Horányi, M. 2010, *Geophys. Res. Lett.*, 37
- Poppe, A. R. 2016, *Icarus*, 264, 369
- Quinten, M., Kreibig, U., Henning, T., & Mutschke, H. 2002, *Appl. Optics*, 41, 7102
- Reuter, D. C., Stern, S. A., Scherrer, J., et al. 2008, *SSRv*, 140, 129, doi: [10.1007/s11214-008-9375-7](https://doi.org/10.1007/s11214-008-9375-7)
- Rice, K. 2014, *Challenges*, 5, 296, doi: [10.3390/challe5020296](https://doi.org/10.3390/challe5020296)
- Rogers, G., Schwinger, M., Kaidy, J., et al. 2006, *Autonomous Star Tracker Performance for the New Horizons Mission* (American Institute of Aeronautics and Astronautics). <https://doi.org/10.2514/6.2006-6383>

- Sano, K., Kawara, K., Matsuura, S., et al. 2015, *ApJ*, 811, 77, doi: [10.1088/0004-637X/811/2/77](https://doi.org/10.1088/0004-637X/811/2/77)
- Singer, L. P., Chen, H.-Y., Holz, D. E., et al. 2016, *ApJL*, 829, L15, doi: [10.3847/2041-8205/829/1/L15](https://doi.org/10.3847/2041-8205/829/1/L15)
- Stern, A., & Spencer, J. 2003, *Earth Moon and Planets*, 92, 477, doi: [10.1023/B:MOON.0000031962.33024.33](https://doi.org/10.1023/B:MOON.0000031962.33024.33)
- Stern, S. A. 1996, *Astron. Astrophys.*, 310, 999
- Stern, S. A., Slater, D. C., Scherrer, J., et al. 2008, *SSRv*, 140, 155, doi: [10.1007/s11214-008-9407-3](https://doi.org/10.1007/s11214-008-9407-3)
- Stone, E., Alkalai, L., Friedman, L., et al. 2015, *Science and Enabling Technologies for the Exploration of the Interstellar Medium*, Tech. rep., Keck Institute for Space Studies
- Street, R. A., Udalski, A., Calchi Novati, S., et al. 2016, *ApJ*, 819, 93, doi: [10.3847/0004-637X/819/2/93](https://doi.org/10.3847/0004-637X/819/2/93)
- Sullivan, P. W., Winn, J. N., Berta-Thompson, Z. K., et al. 2015, *ApJ*, 809, 77, doi: [10.1088/0004-637X/809/1/77](https://doi.org/10.1088/0004-637X/809/1/77)
- Sumi, T., & Penny, M. T. 2016, *ApJ*, 827, 139, doi: [10.3847/0004-637X/827/2/139](https://doi.org/10.3847/0004-637X/827/2/139)
- Szalay, J. R., Piquette, M., & Horányi, M. 2013, *Earth Planets Space*, 65, 1145
- Toller, G., Tanabe, H., & Weinberg, J. L. 1987, *A&A*, 188, 24
- Toller, G. N. 1983, *ApJL*, 266, L79, doi: [10.1086/183982](https://doi.org/10.1086/183982)
- Totani, T., Yoshii, Y., Iwamuro, F., Maihara, T., & Motohara, K. 2001, *ApJL*, 550, L137, doi: [10.1086/319646](https://doi.org/10.1086/319646)
- Tsapras, Y., Hundertmark, M., Wyrzykowski, L., et al. 2016, *MNRAS*, 457, 1320, doi: [10.1093/mnras/stw023](https://doi.org/10.1093/mnras/stw023)
- Tsumura, K., Matsumoto, T., Matsuura, S., Sakon, I., & Wada, T. 2013, *PASJ*, 65, 121, doi: [10.1093/pasj/65.6.121](https://doi.org/10.1093/pasj/65.6.121)
- Tyson, J. A. 1995, in *Extragalactic Background Radiation Meeting* (Ed. Calzetti, D. et al.) 103-133, ed. D. Calzetti, M. Livio, & P. Madau, 103-133
- Valenti, S., David, Sand, J., et al. 2017, *ApJL*, 848, L24, doi: [10.3847/2041-8213/aa8edf](https://doi.org/10.3847/2041-8213/aa8edf)
- Vanderburg, A., & Johnson, J. A. 2014, *PASP*, 126, 948, doi: [10.1086/678764](https://doi.org/10.1086/678764)
- Verbiscer, A. J., Skrutskie, M. F., & Hamilton, D. P. 2009, *Nature*, 461, 1098
- Vitense, C., Krivov, A. V., Kobayashi, H., & Löhne, T. 2012, *Astron. Astrophys.*, 540
- Vitense, C., Krivov, A. V., & Löhne, T. 2010, *Astron. Astrophys.*, 520
- Warren, S. G. 1984, *Appl. Optics*, 23
- Weaver, H. A., Gibson, W. C., Tapley, M. B., Young, L. A., & Stern, S. A. 2008, *SSRv*, 140, 75, doi: [10.1007/s11214-008-9376-6](https://doi.org/10.1007/s11214-008-9376-6)
- Weinberg, J. L., Hanner, M. S., Beeson, D. E., DeShields, II, L. M., & Green, B. A. 1974, *J. Geophys. Res.*, 79, 3665, doi: [10.1029/JA079i025p03665](https://doi.org/10.1029/JA079i025p03665)
- Wright, E. L. 2001, *ApJ*, 553, 538, doi: [10.1086/320942](https://doi.org/10.1086/320942)
- . 2004, *NewAR*, 48, 465, doi: [10.1016/j.newar.2003.12.054](https://doi.org/10.1016/j.newar.2003.12.054)
- Wyrzykowski, L., Skowron, J., Kozłowski, S., et al. 2011, *MNRAS*, 416, 2949, doi: [10.1111/j.1365-2966.2011.19243.x](https://doi.org/10.1111/j.1365-2966.2011.19243.x)
- Yee, J. C., Gould, A., Beichman, C., et al. 2015, *ApJ*, 810, 155, doi: [10.1088/0004-637X/810/2/155](https://doi.org/10.1088/0004-637X/810/2/155)
- Zemcov, M., Immel, P., Nguyen, C., et al. 2017, *Nature Communications*, 8, 15003, doi: [10.1038/ncomms15003](https://doi.org/10.1038/ncomms15003)
- Zemcov, M., Smidt, J., Arai, T., et al. 2014, *Science*, 346, 732, doi: [10.1126/science.1258168](https://doi.org/10.1126/science.1258168)
- Zhu, W., Udalski, A., Huang, C. X., et al. 2017a, *ApJL*, 849, L31, doi: [10.3847/2041-8213/aa93fa](https://doi.org/10.3847/2041-8213/aa93fa)
- Zhu, W., Huang, C. X., Udalski, A., et al. 2017b, *PASP*, 129, 104501, doi: [10.1088/1538-3873/aa7dd7](https://doi.org/10.1088/1538-3873/aa7dd7)